Title

The lysosomal GPCR-like protein GPR137B regulates Rag and mTORC1 localization and activity

Journal

Nature Cell Biology, 21(5)

ISSN

1465-7392

Authors

Gan, Lin
Seki, Akiko
Shen, Kimberle
et al.

Publication Date

2019-05-01

DOI

10.1038/s41556-019-0321-6

Peer reviewed

The lysosomal GPCR-like protein GPR137B regulates Rag and mTORC1 localization and activity

Lin Gan[1#], Akiko Seki[1#], Kimberle Shen[2], Harini Lyer[2], Kyuho Han[1], Arnold Hayer [1], Roy Wollman[3], Xuecai Ge[1], Jerry Lin[1], Gautam Dey[1], William S. Talbot[2], Tobias Meyer[1]

[1]Department of Chemical and Systems Biology, Stanford University

[2]Department of Developmental Biology, Stanford University

[3]Present address: Department of Chemistry and Biochemistry, Division of Biology, Section for Cellular and Developmental Biology, University of California, San Diego.

#These authors contributed equally to this work.

Mammalian cell growth is controlled by a lysosomal signaling complex containing Rag small GTPases and mTORC1 kinase. Here we carried out a microscopy-based genome-wide human siRNA screen and discovered a lysosome-localized G-protein coupled receptor (GPCR)-like protein, GPR137B, that interacts with Rag GTPases, increases Rag localization as well as activity, and thereby regulates mTORC1 translocation and activity. High GPR137B expression can recruit and activate mTORC1 in the absence of amino acids. We found that activated Rag dissociates more rapidly from lysosomes and GPR137B regulates this Rag dissociation rate, suggesting that GPR137B controls a Rag activation-dissociation cycle. Rag and Raptor are able to remain associated in the cytoplasm, suggesting Rag bound mTORC1 complexes persist after dissociation from lysosomes. GPR137B knockout cells exhibited defective autophagy and an expanded lysosome compartment, similar to Rag knockout cells. GPR137B mutant zebrafish also had an expanded lysosome compartment in microglia and upregulation of TFEB targets' expression, like RagA mutant zebrafish. Thus, GPR137B is a GPCR-like lysosomal regulatory protein that controls dynamic Rag and mTORC1 localization and activity as well as lysosome morphology.

Keywords: mTORC1, lysosomes, Rag, nutrient sensing, mTOR signaling

INTRODUCTION

Cells regulate growth, autophagy and metabolism by employing a lysosomal regulatory complex consisting of heterodimers of Rag small GTPase (one RagA/B protein paired with one RagC/D protein)[1–3] and a cytoplasmic regulatory complex mTORC1 containing the protein kinase mTOR and an adapter protein Raptor [4,5] (Fig. 1a). Rag dimers are anchored to the lysosomes and activated by a lysosome-localized Ragulator adapter complex [6,7], and inactivated by a GATOR1 complex that stimulates the hydrolysis of GTP in active RagA/B-GTP to produce inactive RagA/B-GDP [8,9]. Amino acids, glucose and possibly other nutrient signaling pathways increase the activity of Rags and thereby recruit mTORC1 to lysosomes [4,10,11]. Once localized at lysosomes, the kinase activity of mTORC1 is regulated by growth factors and insulin that control mTORC1 through a PI3K-Akt-TSC2-Rheb signaling pathway and other mechanisms [12–15]. Most of the known regulators of mTORC1 are not unique to lysosomes or only membrane-associated. Only two transmembrane proteins, the proton pump v-ATPase and the arginine transporter SLC38A9, have been shown to regulate mTORC1 [16–18], suggesting that additional dedicated transmembrane proteins may exist that are unique to lysosomes and regulate Rag activity.

Using genetic approaches to investigate the function of Rags and Rag regulators has been challenging due to the complexity of the phenotypes observed in gene knockout experiments. Recent knockout studies suggested that mTORC1 regulation by Rags can be compensated for by other mechanisms, but phenotypes of lysosome compartment expansion and autophagosomes/autolysosomes accumulation tended to persist [10,19–21]. In addition, knockout of two Rag regulators, WDR24 and LAMTOR1, showed similar lysosome and autophagy defects [22,23]. Together, these studies uncovered important functions of Rags in lysosome/autophagy regulation that cells and organisms cannot compensate for.

Here we took an unbiased approach and used a genome-wide siRNA screen to identify additional regulators of lysosomal mTORC1 localization and activity. We identified GPR137B, a lysosome-localized GPCR-like protein with unknown function, as a regulator that can recruit mTORC1 to lysosomes and activate mTORC1. We show that GPR137B regulates mTORC1 through Rag proteins in two ways: by interacting with Rag proteins and increasing Rag concentration at lysosomes and by increasing the GTP-loaded, active state of lysosomal RagA, which causes a recruitment of mTORC1 and an accelerated dissociation of active Rags from lysosomes. Active Rags can still be bound with Raptor after lysosome dissociation. Most known components of the Ragulator/GATOR/Rag complex that regulate mTORC1 translocation are not transmembrane proteins, it is intriguing that GPR137B is the first lysosomal transmembrane protein that can activate Rag and recruit mTORC1 even in the absence of amino acids. Finally, we show that knockout of GPR137B in human cells results in a similar expansion of the lysosome compartment and increased autophagy markers as observed in RagA/B knockout MEFs and cardiomyocytes [19]. We further observed an expanded lysosomal compartment phenotype in microglial cells *in vivo* in GPR137B mutant zebrafish and upregulation of expression of TFEB targets, similar to RagA mutant fish. Together, our study introduces a GPCR-like activator of lysosomal Rag and mTORC1 signaling that regulates the dynamic

exchange of active Rags at lysosomes and provides a potential therapeutic target to regulate mTORC1 activity.

RESULTS

Human siRNA screen identifies a lysosome-localized GPCR-like protein as a regulator of mTORC1

We sought to identify new mediators of amino acid signaling to mTORC1 by screening through 21,041 pools of Dharmacon siRNAs in non-transformed human fibroblasts (Hs68). Each pool consisted of 4 siRNAs targeting an individual gene in the human genome. Our microscopy-based assay monitored the amino acid-triggered increase in phosphorylation of the ribosomal protein S6 (rpS6) at residue 240 and 244 (Fig. 1a, b) [24,25]. Known inhibitors of the mTORC1 pathway suppress this phosphorylation (Supplementary Fig. 1a). The assay had a high signal-to-noise ratio and reproducibly captured roughly an equal number of positive and negative regulators such as the mTORC1 activator Rheb and the suppressor TSC2 (Fig. 1c and Supplementary Fig. 1b) with significant effects for over 2000 siRNA pools (Fig. 1c, Supplementary Table 1), including many known regulators of mTORC1 signaling (Fig. 1c, arrows). We tested the screening results with individual siRNAs and narrowed our focus on 427 high confidence candidates (Supplementary Fig. 1c). Ingenuity pathway analysis showed that genes associated with insulin/growth factor, PI3K/AKT, ERK/MAPK, Hedgehog, p53, AMPK, and cell cycle signaling pathways were significantly enriched in the set (Supplementary Fig. 1d), confirming that growth, proliferation and stress are linked to mTORC1 signaling. This analysis also linked potential additional regulatory modules to mTORC1 signaling such as the glycine cleavage pathway (Supplementary Fig. 1d, Table 2).

Since amino acid-induced translocation of mTORC1 to lysosomes is a key step in the activation process [6,8], we used an automated microscopy assay to monitor mTORC1 translocation by quantifying the co-localization between the lysosome marker Lamp2 and mTOR. To exclude indirect regulators that control amino acids uptake from outside the cell, we first starved cells and then induced a transient increase in intracellular amino acids by inhibiting protein translation using cycloheximide [26] (Fig. 1d and Supplementary Fig. 1e). Using this assay, we screened for effects caused by the knockdown of each of the 427 candidate genes. A small subset of hits significantly reduced mTOR translocation to lysosomes as well as rpS6 phosphorylation (Fig. 1e, f), consistent with the interpretation that only a subset of genes regulates mTORC1 translocation while most genes regulate mTORC1 after or independent of mTORC1 lysosome translocation. Fig. 1g shows a list of 15 identified genes ranked according to the strength of suppression of mTOR localization to lysosomes. Among them, the poorly understood or uncharacterized candidate genes include transporters, an anti-apoptotic factor TIAF1 and a F-box DNA helicase, suggesting that other nutrient or metabolite sensing, as well as cellular stress such as DNA replication stress, regulate mTORC1 translocation. RagC was the top hit regulating mTOR translocation in the screen, confirming the importance of Rag GTPases

in mTORC1 recruitment. We focused our subsequent analysis on another top hit, GPR137B, because it has been shown to be lysosome-localized [27] and because it is a predicted 7-transmembrane protein with a low sequence homology to G-protein coupled receptors (GPCRs) (Fig. 2a).

GPR137B regulates lysosome localization and activity of mTORC1

Consistent with the reported lysosome localization of GPR137B, we found that GPR137B-YFP colocalized with the lysosomal marker Lamp2. GPR137B also colocalized with mTOR after amino acid stimulation (Fig. 2b). To quantify the relative lysosomal localization of mTOR, we developed an automated analysis for mTOR localization and translocation based on a binary lysosome mask and local background subtraction. Two independent individual siRNAs used in two cell types (Hs68 and HeLa cells) confirmed our screening result that knocking down GPR137B reduces mTOR translocation to lysosomes as well as rpS6 phosphorylation (Fig. 2c, d and Supplementary Fig. 2a-c for verification of knockdown and rescue). Timecourse analysis revealed that GPR137B knockdown reduces mTORC1 basal activity as measured by rpS6 phoshorylation in nutrient-replete cells as well as mTORC1 re-activation120min post amino acid addback in starved cells(Supplementary Fig. 2d), suggesting it does not simply cause a delay in mTORC1 re-activation. Translocation analysis further showed that GPR137B is a limiting positive regulator of translocation since its overexpression strongly increased mTOR translocation in the absence and weakly in the presence of amino acids (Fig. 2e, f). Strikingly, in the absence of amino acids, high expression of GPR137B induced lysosome translocation of mTOR close to the level reached by amino acid stimulation (Fig. 2f; control experiments in Supplementary Fig. 2e). Finally, GPR137 and GPR137C, two genes homologous to GPR137B, likely have a similar role in regulating mTORC1 since we found that they were also lysosome-localized (Fig. 2g) and both increased mTOR translocation to lysosomes when overexpressed (Supplementary Fig. 2f, g). Together, these results suggest that GPR137B is part of a family of lysosome-localized GPCR-like proteins that regulate mTORC1 translocation to lysosomes.

An important role of mTORC1 is to inhibit autophagosome formation through phosphorylation of the ULK1-mATG13-FIP200 complex [28]. Upon amino acid deprivation, autophagy is upregulated by relieving this mTORC1-mediated inhibition. Consistent with a role of GPR137B in regulating mTORC1 activity, knocking down GPR137B increased autophagy, as indicated by an increase in the number of LC3-GFP puncta per cell (Fig. 2h). Upregulation of LC3-GFP could be caused by an increase in autophagy induction or autophagosome accumulation due to flux defects. p62 is an ubiquitin-binding protein that is degraded by autophagy and will accumulate if autophagy flux is reduced[50] and previous studies have used p62 as read out of autophagy flux defects in the mTOR/Rag pathway[10,19–21]. We observed a marked upregulation of p62 in GPR137B knockdown cells and the p62 puncta tend to co-localize with LC3-GFP puncta (Fig. 2l,m), suggesting that autophagy flux defects contribute significantly to the increase in LC3-GFP in GPR137B knockdown cells. Another key role of mTORC1 is the phosphorylation of 4E-BP1, a critical mTORC1 substrate and regulator of protein synthesis and cell size [29–31]. Overexpression of GPR137B-YFP in cells starved of amino acids was sufficient to

increase the phosphorylation of 4E-BP1 close to the level reached by amino acid stimulation (Fig. 2i and Supplementary Fig. 2h for controls). Furthermore, biochemical analysis confirmed that knockdown of GPR137B suppresses phosphorylation of S6K and 4E-BP1 similarly to a knockdown of RagA/C and overexpression of GPR137B increased their respective phosphorylation even in the absence of amino acids, and this increased phosphorylation is abolished upon rapamycin treatment (Fig. 2j, k). The rapamycin-sensitive phosphorylation of S6K at pT389 promoted by GPR137B suggest that GPR137B mediates its effects specifically through mTORC1. Furthermore, in serum-starved cells expressing GPR137B, there was no statistically significant increase either in mTORC1 translocation or mTORC1 activity as measured by phosphorylation of 4EBP1, compared to control cells(Supplementary Fig. 2i,j), suggesting that GPR137B regulation of mTORC1 is more specific to amino acid signaling. Thus, GPR137B regulates amino acid-induced mTORC1 translocation to lysosomes and mTORC1 activity, and has likely a functional role in regulating autophagy as well as protein synthesis and cell size through regulation of S6K and 4E-BP1.

GPR137B regulates mTORC1 localization and activity through Rag GTPases

We used RagA/B knockout MEFs [19] to determine whether GPR137B signals to mTORC1 through Rags. Markedly, stable expression of GPR137B could not restore mTORC1 translocation in Rag A/B knockout MEFs (Fig. 3a, b,c; Supplementary Fig. 3a), arguing that GPR137B regulates mTORC1 localization and activity through Rags.

Furthermore, when we overexpressed constitutively active RagA/C (RagA-Q66L, RagC-T75N) [4] in HeLa cells, knockdown of GPR137B did not alter the increased lysosomal mTORC1 localization (Fig. 3d), suggesting that GPR137B no longer regulates mTORC1 translocation once Rag has been activated. In an independent strategy to activate endogenous Rags, we overexpressed GPR137B in HEK293E cells deficient of the GATOR1 component Nprl3 [8]. Loss of the GAP activity for RagA has been shown to cause RagA activation as well as lysosome localization and activation of mTORC1. While the wildtype cells showed a GPR137B expression-mediated increase in mTORC1 translocation, GPR137B did not cause additional mTORC1 translocation in the knockout cells (Fig. 3e). Together, these results argue that GPR137B signals through Rag GTPases to regulate mTORC1 translocation.

GPR137B interacts with Rags and increases the lysosomal localization of RagA

To understand the mechanism of Rag regulation by GPR137B, we probed the binding interactions of GPR137B with some of the known components of the mTORC1 regulatory machinery localized at lysosomes. In HEK293T cells, we found that GPR137B co-immunoprecipitated with mTOR, Raptor, and RagA, as well as with Sestrin2 (Fig. 4a, Supplementary Fig. 3b). We were unable to observe interactions with components of Ragulator or GATOR complexes that we tested nor with SLC38A9 (Supplementary Fig. 4c). Interestingly, when we co-expressed two GPR137B constructs with different tags, we observed an apparent amino acid-stimulated interaction of GPR137B with itself that is dependent on the presence of Rags (Fig. 4b), suggesting that GPR137B is part of an amino acid-regulated multi-protein lysosomal signaling complex that contains more than one GPR137B protein. To probe whether

this self-interaction is dependent on the activation of Rags, we co-expressed wildtype, dominant negative or constitutively-active Rag pairs in Rag A/B knockout MEFs, and observed no different in the amount of GPR137B co-immunoprecipitating with itself (Fig 4c and Supplementary Fig 4d), suggesting this self-interaction of GPR137B is not a result of Rag activation in response to amino acids. Control experiments using the unrelated lysosomal transmembrane protein Npc1 instead of GPR137B did not pull down mTOR or Rag, suggesting that the interactions are specific for GPR137B (Supplementary Fig. 4a). Furthermore, when we tested for the interaction between GPR137B and mTOR in MEF cells deficient in RagA/B, GPR137B failed to interact with mTOR (Fig. 4b; Supplementary 3b). Notably, the binding interactions of GPR137B with mTOR, Raptor and GPR137B itself were all amino acid sensitive, but the interaction of GPR137B with RagA was not (Fig. 4a, Supplementary Fig. 4b, c). These interaction data suggest that RagA/B is required to assemble a GPR137B-RagA/B-mTORC1 signaling complex at lysosomes and that GPR137B regulates mTORC1 by binding RagA.

Since we observed an interaction between GPR137B and Sestrin2 (Fig. 4a), we determined whether GPR137B signals through Sestrin2 which has been reported to function as a leucine sensor that regulates RagA through a GATOR2 complex that represses GATOR1 [32–35] and/or as a direct regulator of RagA [36]. We used triple Sestrin1/2/3 knockout cells [34] that have higher basal lysosome localization of mTORC1. However, overexpression of GPR137B could still increase mTOR translocation to lysosomes in these cells (Fig. 4d), arguing that GRP137B can regulate Rag and mTORC1 independent of Sestrins and the Sestrin-associated leucine sensing pathway. Therefore we did not investigate the role of Sestrin2 further.

Given that GPR137B can interact with Rags, we next tested whether GPR137B regulates the localization of Rags analogous to Ragulator proteins that anchor Rags to lysosomes. We first confirmed that expression of GPR137B, but not of Lamp1, caused an expression-dependent increase in mTORC1 translocation in both the absence and presence of amino acids (Fig. 4e, left panels). Markedly, however, increased GPR137B expression also caused a small but significant increase in RagA localization at lysosomes (Fig. 4e, right panels; see Supplementary Fig. 4e for RagC data). We further validated the regulation of Rag localization by showing that siRNA against GPR137B causes a reduction in the amount of lysosomal RagA (Fig. 4f) and RagC (Fig. 4g). Knockdown of the Ragulator component LAMTOR2 was included as a reference, showing that the effect by GPR137B is modest in comparison. Furthermore, GPR137B does not seem to induce increased recruitment of Rag or increased mTORC1 activity in cells depleted of Ragulator. siLAMTOR33 treated cells showed significantly reduced RagA and mTOR localization at the lysosome, and co-expressing either Lamp1 or GPR137B showed very little difference in the RagA lysosome localization(Supplementary Fig.4f,g). Thus, GPR137B can interact with Rags and increase lysosomal Rag localization in a Ragulator-dependent manner. Taken together with our data in Fig. 3, the binding and localization results suggest that GPR137B regulates both Rag localization as well as RagA GTP loading and activity.

GPR137B increases Rag activity to recruit mTORC1

We used the selective binding of mTORC1 to RagA-GTP over RagA-GDP as a measure to determine whether RagA is in the active GTP bound state (Sancak et al., 2008). Consistent with

a role of GPR137B in regulating RagA GTP loading, knockdown of GPR137B inhibits the interaction between RagA and both mTOR and Raptor (Fig. 5a, Supplementary Fig 5a,b) while overexpression of GPR137B increases the interaction between RagA and mTOR and Raptor (Fig. 5b, Supplementary Fig 5c,d). Markedly, when additional GPR137B is expressed in cells, the binding of RagA and Raptor is already increased in the absence of amino acids, suggesting that GPR137B can increase RagA GTP loading even in the absence of amino acids (Fig. 5b, Supplementary Fig 5c,d), consistent with the immunofluorescence data (Fig. 2f).

We next determined whether co-expression of Rag and GPR137B induces synergistic mTORC1 translocation to investigate whether additional rate-limiting co-factors are needed. We used the stochastic nature of transient co-expression to select cells that have different levels of fluorescently-tagged RagC and GPR137B. We expressed RagC alone because expression of RagC causes a corresponding increase in endogenous RagA abundance [37]. When we co-expressed RagC together with Lamp1 control, we did not find significant increases in mTORC1 translocation, suggesting that Rags, at any level, mediate only minimal basal mTORC1 recruitment under low amino acid conditions (Fig. 5c, d). In contrast, the diagonal activity increases in the mTORC1 translocation heatmap shows a marked synergy between Rag and GPR137B in recruiting mTORC1, meaning that a lower level of GPR137B is needed to cause mTORC1 translocation at higher RagC expression, and vice versa (Fig. 5c, bottom panel). In control experiments, co-expression of GPR137B and an unrelated small GTPase Rap2A does not produce synergy (Supplementary Fig. 6a). The synergy between GPR137B and Rag and the high level of mTORC1 translocation reached in cells co-expressing both proteins (Fig. 5d) makes it unlikely that additional rate-limiting factors are needed for GPR137B to regulate the activity of Rags. To further investigate whether GPR137B causes mTORC1 translocation through promoting Rag GTP loading, we transiently co-expressed GPR137B with wildtype or dominant-negative RagA/C pair (RagA T21N/RagC Q120L) in RagA/B null MEFs, which had no mTORC1 translocation when stably-expressing GPR137B alone (Fig 3b,c), but displayed robust mTORC1 translocation even in the absence of amino acids when co-expressed with wildtype RagA/C , and significantly reduced mTORC1 translocation when co-expressed with dominant-negative RagA/C pair (Fig5e, right panels, Supplementary Fig 6d), suggesting the change in nucleotide status of Rags to GTP is partially required for GPR137B to mediate its effect on mTORC1 translocation. The residual mTORC1 translocation seen at significantly higher GPR137B levels could be due to excess GPR137B compensating for the reduced binding ability of DN RagA/C pair for mTORC1), suggesting that GPR137B maybe also signal through other Rag interactions, such as Rag heterodimer stabilization or mTORC1/Rag complex stabilization at the lysosomes. This would be consistent with our previous observation that GPR137B also increases RagA localization at the lysosomes (Fig.4e) and forms a multi-protein complex with mTORC1/Rag(Fig.4b). As a control, Lamp1 co-expressed with wildtype RagA/C caused low amount of mTORC1 translocation at high Rag A/C levels but did not display any synergistic effects as seen with GPR17B co-expression (Fig 5e top panels), and Lamp1 co-expressed with dominant-negative RagA/C pair did not show any mTORC1 translocation (Fig5e, bottom left panel). All heatmaps included most values in the wells and the comparison of wildtype and dominant negative RagA/C expression levels was carefully calibrated by an endogenous RagA

antibody (Supplementary Fig 6b,c). Together with the finding that GPR137B regulates the binding interaction between RagA and mTORC1, these results support the hypothesis that the level of GPR137B regulates RagA GTP loading and activity in addition to RagA localization.

Photobleaching recovery analysis suggests that GPR137B regulates a cycle of dynamic activation and dissociation of lysosomal Rags

In addition to lysosome recruitment of Rags by GPR137B, Fig. 4e also showed an unexpected amino acid-triggered reduction in Rag localization at lysosomes. When we compared the kinetics of Rag and mTOR localization changes at lysosomes after amino acid stimulation, we were surprised to find that both endogenous RagA and RagC dissociated from lysosomes in response to amino acids with kinetics that paralleled the increase in mTOR translocation to lysosomes (Fig. 6a-c). We next made use of previous studies that showed a negative feedback whereby mTORC1-mediated Rag ubiquitination reduces lysosomal localization of mTORC1 with a delay after amino acid stimulation [38,39]. Indeed, when we treated amino acid-stimulated cells with rapamycin to suppress this negative feedback loop, more mTOR translocated to lysosomes as expected. Markedly, we also found that a greater fraction of RagA and C dissociated from lysosomes, also with the same kinetics as mTOR translocation to lysosomes (Fig. 6d-f). The anti-correlated changes in the kinetics and relative amplitude of mTOR and Rag localization suggest that recruitment of mTORC1 and dissociation of Rags are connected events.

Based on the observation that Rag activity might regulate its localization, we tested whether active GTP-loaded RagA have a faster exchange rate from lysosomes compared to inactive GDP-loaded RagA. We overexpressed constitutively active or dominant negative RagA paired with fluorescently-tagged wildtype RagC and performed fluorescence photobleaching recovery analysis to measure the steady state exchange rate of RagC from lysosomes. Since RagA and C form a dimer, one can use the RagC dissociation rate as an indirect measure of the dimer dissociation rate. Markedly, the dissociation rate of dominant negative RagA/C was slower compared to constitutively active RagA/C (Fig. 6g, h), suggesting that GTP loading of RagA lowers the affinity of RagA for lysosomes and accelerates RagA/C dissociation from lysosomes. This is also consistent with the previous finding that the affinity of Ragulator for Rag A/B is lower in the GTP-loaded, active state of RagA/B [7]. Our results are consistent with a recent publication showing Rags cycle on and off the lysosomes depending on their activation state[51].

The differential dissociation kinetics of mutant RagA proteins allowed us to use wildtype RagA/C expressing cells to test whether the exchange rate of Rags is regulated by amino acids. Indeed, lysosomal RagC exchanges more rapidly after amino acid stimulation (Fig. 6i). This is consistent with the interpretation that amino acids trigger RagA to become GTP-loaded to recruit mTORC1 and also accelerate its own dissociation from lysosomes, leading to overall reduced Rag localization at lysosomes. When we expressed GPR137B in amino acid-starved cells, we found a small but significant increase in the RagC exchange rate (Fig. 6j, k), consistent with the interpretation that GPR137B increases GTP loading of RagA as well as the rate of RagA/C dissociation already in the absence of amino acids. Conversely, when we knocked-down GPR137B, there was a small but significant decrease in the RagC exchange rate (Fig. 6l,m) and when we expressed GPR137B in Nprl3-/- HEK293E cells where Rags are presumed to be mostly

GTP-loaded [8] and there was no further effect of GP137B on mTORC1 translocation(Fig. 3e), there was no statistically-significant difference of the RagC exchange rate from control cells (Supplementary Fig.6e). Taken together, these results suggest that GPR137B regulates Rag turnover at the lysosome through Rag GTP loading.

Together, the regulated dissociation of RagA from lysosomes that we discovered can potentially be interpreted in the context of a previous observation that mTORC1 is active not only at lysosomes but also at other cellular locations [40], and that the binding between Ragulator and Rag is reduced after amino acid stimulation [7]. Since mTORC1 complexes that dissociate from lysosomes can be active [41], our finding of a GPR137B-regulated dissociation rate of RagA/C suggests that GPR137B regulates Rags in two steps: first by activating lysosomal RagA which recruits mTORC1 to lysosomes for a short time period, second by enabling Rag dissociation from lysosomes possibly as an active or activatable Rag/mTORC1 complex in which bound Rags keeps mTORC1 transiently active or primed in the cytosol. To test whether the dynamic cycling of Rags result in a cytoplasmic pool of Rag bound mTORC1 complexes, we fused the C1 domain from rat PKC protein[52] to RagC and co-expressed Raptor, constitutively-active RagA and a CAAX membrane marker in HEK293T cells. We recruited C1 domain-tagged RagC to the plasma membrane using 3uM PMA and observed a concomitant recruitment of Raptor to the plasma membrane as well (Fig. 7a,b). To exclude artifacts of overexpression, we analyzed cells that only expressed Raptor at levels barely above background (examples in Supplementary Fig. 7c) and showed that the plasma membrane to cytoplasmic intensity ratio of Raptor post PMA addition is consistently higher for cells expressing C1-tagged RagC than a wildtype RagC (Fig. 7c). As controls, we verified that C1-domain tagged RagC can recruit wildtype RagA to the plasma membrane (Supplementary Fig. 7a) and that neither C1-domain tagged RagC nor Raptor co-localizes with Lamp2 at the plasma membrane (Supplementary Fig. 7b). This observation suggests their plasma membrane translocation is unlikely due to lysosomes bearing Rag and Raptor being pulled to the plasma membrane and fusing. Given the finding [51] that Rag and mTORC1 dissociate together from the lysosomes, our results suggest that Rag-mTORC1 can remain associated in the cytoplasm after dissociation and Rag-mTORC1 might dynamically cycle together as a way to regulate their activation. Thus GPR137B regulation of this Rag activation-dissociation cycle could be an important part of a dynamic activation

mechanism for lysosomal Rag and mTORC1 signaling. Mutational analysis in human cells and zebrafish provides evidence that GPR137B regulates lysosome morphology through Rag

As discussed in the introduction, cells can adapt to the loss of Rag signaling and have normal mTORC1 activity in a Rag-independent manner, such as in cardiomyocytes from RagA/B double knockout mice and in microglia from RagA mutant zebrafish (Zebrafish lack RagB). Nevertheless, this adaptation is not complete, as knockouts of Rag and Rag regulators in different cell types and species all have similar lysosomal and autophagy defects [19,21–23]. For example, Rag A/B knockout MEFs[19], knockouts of two Rag regulators, WDR24 and LAMTOR1[22,23] also showed an increased Lamp1/LysotrackerRed positive compartment and abnormal accumulation of autophagomes/autolysosomes that stained positive for LC3 or Atg8a. To determine whether knockout of GPR137B causes a similar phenotype as the loss of Rag activity, we used HapI knockout cells deleted for GPR137B or its potential functional homolog, GPR137. Both GPR137B and GPR137 HapI knockout cells showed expanded lysosome compartment as measured by larger LysotrackerGreen positive puncta (Fig. 8a, b), as well as increased autophagosomes/autolysosomes as measured by increased LC3B puncta per cell (Fig. 8c), similar to Rag or Rag regulator knockouts. In addition, in both cell lines, the lysosomal localization of endogenous RagA was decreased, similar to the GPR137B knockdown result (Fig. 8e). Nevertheless, mTORC1 translocation to lysosomes could still be regulated by amino acids (Fig. 8d, Supplementary Fig. 8a). Together, the similar cellular effects of GPR137B knockout and Rag or Rag regulator knockouts are consistent with the interpretation that a main role of GPR137B is regulation of Rag activity.

To investigate the function of GPR137B in vivo, we identified homologs of this gene in zebrafish. The zebrafish genome encodes four homologs of GPR137B: *gpr137ba, gpr137bb, gpr137c,* and *gpr137*. Of these four zebrafish GPR137B homologs, Gpr137ba is most similar to the human GPR137B protein (Supplementary Fig. 8e and f). The hypothesis that Gpr137B activates RagA predicts that there should be phenotypic similarities between *rraga* mutants and mutants in one or more of the four *gpr137* genes. We generated mutants for three of the annotated genes, *gpr137ba, gpr137c,* and *gpr137,* using TALEN-targeted nucleases(Supplementary Fig 8b). *gpr137bb* was annotated more recently, and we have analyzed its function in transient CRISPR experiments. Our preliminary studies revealed similarities between mutants for *rraga* and *gpr137ba*, but not *gpr137c* or *gpr137* mutants, or wildtype fish injected with CAS9 and guide RNA for *gpr137bb.* We therefore focused additional analyses on *gpr137ba* mutants.

Zebrafish *rraga* mutants have abnormal microglia with expanded lysosomes (Shen et al., 2016), so we examined these specialized brain macrophages in *gpr137ba* mutant zebrafish. Microglia in *gpr137ba* mutants had an expansion of the lysosomal compartment, with large

clusters of LysoTracker Red positive puncta, similar to *rraga* mutant zebrafish (Fig. 7h, i). Homozygous *gpr137ba* mutant fish had otherwise normal morphology and were viable as adults (Supplementary Fig. 8c). Microglial cell numbers and markers of autophagy, such as LC3B and p62, were unchanged in *gpr137ba* mutants relative to controls (Fig. 7f-g, Supplementary Fig. 8d).

RagA represses the activity of the key lysosomal transcription factor TFEB (Napolitano and Ballabio, 2016), and quantitative real-time PCR studies in zebrafish have demonstrated that transcripts of some TFEB targets are significantly upregulated in *rraga* mutant zebrafish (Meireles et al., 2018; Shen et al., 2016). The hypothesis that GPR137B activates RagA predicts that TFEB targets will be similarly upregulated in *gpr137ba* mutants. To investigate this possibility, we conducted qRT-PCR on larvae from a cross of *gpr137c*$^{+/-}$*; gpr137*$^{+/-}$*; gpr137ba*$^{-/-}$ X *gpr137c*$^{-/-}$*; gpr137*$^{+/-}$*; gpr137ba*$^{+/-}$ adults. Individual fish were genotyped for the *gpr137ba* mutation and pooled, so that one pool of siblings was *gpr137ba*$^{-/-}$ whereas the other pool was *gpr137ba*$^{+/-}$*;* mutations in the other genes were equally represented in both pools. qPCR analysis revealed that some TFEB target genes were significantly upregulated in the *gpr137ba* mutant pool compared to the control pool (Fig 7j), providing evidence that *gpr137ba*, similar to *rraga*, represses the activity of TFEB. Although the levels of p62 protein were similar in immunoblot analysis (Supplementary Fig. 6d), *p62 (sqstm1)* is one of the TFEB target genes whose expression was upregulated in *gpr137ba* mutant pool (Fig 7j). In summary, this analysis revealed some phenotypic similarities between zebrafish mutants for *gpr137ba* and *rraga*, providing evidence that GPR137B regulates the activity of RagA, and as a consequence, the expression of TFEB targets.

Together, while our biochemical and cellular data argues that GPR137B functions as a regulator of lysosomal Rag and mTORC1 localization and activity, the cellular effects of GPR137B knockouts are consistent with incomplete adaptation to a partial or full loss of Rag signaling. Similar to Rag or Rag regulator knockouts, GPR137B knockout human cells retained mTORC1 activity but had expanded lysosome morphology and increased autophagosomes and/or autolysosomes, suggesting that cells fail to compensate for some Rag- and mTORC1- controlled processes when GPR137B or other Rag regulators are lost.

DISCUSSION

Our genome-wide siRNA screen identified GPR137B as a regulator of mTORC1 activation and localization. We focused on GPR137B in part because of its homology to GPCRs, since GPCRs are among the most prominent drug targets in clinical use and since mTORC1 and other lysosomal regulatory pathway components have emerged as promising therapeutic targets for cancer and other diseases [42]. GPR137B has two human homologs that we show also localize to lysosomes and regulate mTORC1 translocation (Fig. 2g; Supplementary Fig. 2f, g). When we performed a sequence homology analysis across multiple eukaryotes [43], we found that genes in the GPR137 family have roots in early eukaryotes with GPR137B homologs being present in

Dictyosteium discoideum, *Monosiga Bervicollis*, many invertebrates and all vertebrates (Supplementary Fig. 8g). Notably, the mTORC1 regulators Rag, Ragulator and GPR137s all have ancient roots but that Ragulator and GPR137s can each individually or both be lost in different evolutionary branches, suggesting that different species may use alternative control mechanisms of Rags and mTORC1.

Our study shows that knockdown and added expression of GPR137B respectively reduces and increases amino acid-triggered mTORC1 translocation to lysosomes and mTORC1 activity. Furthermore, increased expression of GPR137B can activate mTORC1 even under amino acid-starved conditions while also diminishing amino acid sensitivity (Fig. 2f). We provide different lines of evidence that GPR137B regulates mTORC1 through regulation of both the localization and activity of Rags. First, GPR137B no longer regulates mTORC1 lysosome localization in RagA/B knockout cells (Fig. 3b, c). Second, the binding interaction between RagA-GTP and mTORC1 shows that GPR137B regulates the GTP loading state of RagA (Fig. 5a,b). Third, we show that GPR137B interacts with RagA and increases Rag recruitment to lysosomes (Fig. 4e). We also showed synergistic control of mTORC1 translocation by GPR137B and Rags in amino acid-starved cells, where mTORC1 recruitment increases in parallel with increasing concentrations of both Rags and GPR137B (Fig. 5c-d,e,) and significant reduction in mTORC1 translocation when dominant negative Rags are co-expressed, suggesting that GPR137B regulates RagA GTP loading without additional rate-limiting factors.

Finally, our study revealed an unexpected dynamic regulation of RagA, whereby the lysosomal localization of RagA and C is partially and rapidly reduced in response to amino acids. Our photobleaching recovery analysis shows that GTP loading and activation of RagA accelerates the Rag exchange rate from lysosomes (Fig. 6). The correlated recruitment of mTORC1 along with the loss of Rag localization suggested that GPR137B mediates GTP loading of RagA to cause first a recruitment and activation of mTORC1 followed by a potential loss of active Rag/mTORC1 complexes from lysosomes, consistent with a previously proposed dissociation of active mTORC1 [41]. The observation that Rag and Raptor can still associate in the cytoplasm supports this model (Fig.7). This is consistent with the interpretation that GPR137B regulates the formation of active Rag/mTORC1 complexes at lysosomes in an activation cycle whereby the activated Rag/mTORC1 complexes dissociate from lysosomes to activate substrates elsewhere in the cell until Rag is inactivated.

We investigated knockouts of GPR137B in human HapI cells and in developing zebrafish. Previous studies of RagA/B knockouts in mouse and fish showed that cells can compensate and regulate mTORC1 signaling in a lysosome-independent manner when they lose Rags [20,21,44]. However, knockouts of Rags and Rag regulators [22,23] showed a marked increase in accumulation of autophagosomes/autolysosomes as well as lysosomal compartment expansion. Similar to Rag mutant cells, our study showed that knockout of GPR137B, or of GPR137, caused an increase of LC3B positive puncta as well as enlarged lysosome compartments in human cells (Fig. 7a-c). Furthermore, similar to RagA mutant fish, lysosomes were expanded in the microglia of *gpr137ba* zebrafish mutants (Fig. 7h-i), and targets of the lysosomal transcription factor TFEB, which is repressed by RagA, are upregulated in *gpr137ba* mutant zebrafish. Together, these results suggest that GPR137B knockout has overlapping cellular and physiological effects with

knockouts of Rag A/B and of two Rag regulators, consistent with the interpretation that GPR137B has a cellular and organismal function to regulate Rags. Together with the biochemical interaction we observe between RagA and GPR137B and the dual regulation of RagA localization and activity by GPR137B, the GPR137B knockout data further suggest that GPR137B is a key activator of a lysosomal Rag/mTORC1 signaling complex.

Finally, while other transmembrane proteins can regulate mTORC1 signaling, GPR137B is to our knowledge the first whose expression can increase both Rag and mTORC1 localization to lysosomes even in the absence of amino acids, and regulate a dynamic cycle of RagA activation and lysosome dissociation. Given the key roles of mTORC1 signaling in many cancers, it is interesting that a few reports, without providing molecular mechanisms, have suggested a link from GPR137 and GPR137B to different types of cancers[45–48]. Together with our mechanistic results on GPR137B's role in Rag and mTORC1 regulation, this suggests that the three human GPCR-like GPR137 genes are potential novel therapeutic targets for cancers that depend on RagA and/or mTORC1 signaling for growth and survival.

FIGURE LEGENDS

Figure 1: A genome-wide siRNA screen in human primary fibroblasts identifies candidate regulators of amino acid-stimulated mTORC1 translocation and activation

(**a**) Schematic representation of the mTORC1 signaling pathway. rpS6 phosphorylation at 240/244 was used as readout for amino acid-stimulated mTORC1 activation in the siRNA screen. (**b**) *Top*, siRNA screening strategy. *Bottom*, representative immunofluorescence images showing rpS6 phosphorylation at 240/244 in response to amino acid stimulation. Knockdown of the mTOR pathway components Rheb and TSC2 are shown as examples for increased and decreased rpS6 phosphorylation, respectively. Scale bar, 200 μm. (**c**) Genome-wide screen identifies siRNA pools (4 individual siRNAs targeting the same gene) that increase or decrease rpS6 phosphorylation. Z-scores of 21,041 siRNA pools (blue) are plotted over a normally-distributed noise distribution (red). Inset shows reproducibility of Z-scores of two replicate sets. Labeled genes show known mTOR pathway regulators, color-coded according to the schematic in (A). (**d**) Microscopy-based mTORC1 translocation assay based on automated correlation between mTOR and Lamp2 images. Confocal images of Hs68 fibroblasts co-stained for endogenous Lamp2 (green) and mTOR (red). Scale bars, 10μm. (**e**) Lysosome translocation screen identifies candidate siRNAs that decrease mTOR localization to lysosomes as well as rpS6 phosphorylation. (**f**) Sequential selection strategy for candidate regulatory genes (Experimental Procedures). (**g**) Ranked list of 15 candidate

regulators that reduce cycloheximide-induced mTOR translocation confirmed by at least 2 independent siRNAs.

Figure 2: GPR137B regulates mTORC1 translocation to lysosomes and mTORC1 activation

(**a**) Schematic representation of predicted transmembrane domains and topology of GPR137B. (**b**) Confocal image showing colocalization of expressed GPR137B-YFP with endogenous lysosome marker Lamp2 and mTOR in Hs68 cells. Scale bar, 10 μm. (**c**) siRNA knockdown of GPR137B reduces amino acid-induced mTORC1 translocation. Confocal images of Hs68 cells co-stained for endogenous Lamp2 (green) and mTOR (red). Scale bar, 10 □m. (**d**) Correlation analysis between mTOR and Lamp2 localization, and quantification of effects on rpS6 phosphorylation. Effects of siRheb and siRagC are shown for comparison. Error bars are ± SD of population averages; n=6 wells from 3 independent experiments. (**e**) Confocal images of Hela cells showing that GPR137B-YFP overexpression increases amino acid-induced mTOR translocation. HeLa cells were transiently transfected with Lamp1-GFP or GPR137B-YFP, and then starved, re-stimulated with amino acids, fixed and stained with Lamp2 (green) and mTOR antibodies (red). Overexpression of Lamp1-GFP does not increase mTOR translocation in response to amino acids. Scale bars, 10 □m. (**f**) Automated analysis of images such as in (e) using a binary mask for lysosomes showing that amino acids increase mTOR localization at lysosomes approximately 3-fold over that of amino acid-deprived cells. GPR137B-YFP overexpression increases amino acid-induced mTORC1 translocation in the presence or absence of amino acids. High GPR137B expression induces near maximal mTORC1 localization to lysosomes in the absence of amino acids. Error bars are ± SEM of the population average and P values are calculated using two-tailed Student's t test; n=6-8 independent replicates. (**g**) GPR137 and GPR137C are lysosome-localized. Images of HeLa cells transfected with GPR137-YFP or GPR137C-YFP, fixed and stained with antibodies against GFP and Lamp2. Scale bars, 10 □m. (**h**) siRNA knockdown of GPR137B enhances autophagy as measured by an expressed marker of autophagy LC3-GFP. Error bars are ± SD of the population average; n=6 wells from 3 independent experiments. (**i**) GPR137B-YFP expression induces phosphorylation of 4E-BP1 at sites 37/46 even during amino acid starvation. Error bars are ± SEM of the population average; P values are calculated by comparison to untransfected cells in the same well using two-tailed Student's t test; n>5,000 each condition. (**j**) Knockdown of GPR137B inhibits amino acid-induced S6K and 4E-EP1 phosphorylation,. HEK293T cells were transfected with siControl, siGPR137B, and siRagA/C. Phosphorylation of S6K at T389 and 4E-BP1 at T37/46 were examined by western blot. HEK293T cells were amino acid-starved for 1 hour then treated with starvation or amino acid- containing media for 30 min. (**k**) Overexpression of GPR137B desensitizes cells to amino acid withdrawal. GPR137B-3xFLAG or Lamp1-3xFLAG were transiently transfected in HEK293T cells. Cells were amino acid starved for 3

hours then treated with starvation or amino acid containing media for 30 min in the presence or absence of rapamycin. Phosphorylation of S6K was detected by western blot. (**l, m**) siRNA knockdown of GPR137B causes autophagy flux defects as measured by increased p62 levels. Images of HeLa cells transiently-expressing LC3-GFP, treated with siControl or siGPR137B and stained for p62 antibody. Scale bar 20 μm. Bar graph representation of data in (**m**) Error bars are ± SD of the population average and P values are calculated from two-tailed Student's test; n=9 wells from 3 independent experiments.

Figure 3: GPR137B regulates mTORC1 through RagA/B

(**a**) Stable expression of GPR137B-HA in RagA/B-/- MEFs visualized by staining for HA and Lamp2. Scale bar 20 μm. (**b**) mTOR translocation could not be rescued in RagA/B$^{-/-}$ MEFs by stable expression of GPR137B. MEFs starved of amino acids for 60 min and re-stimulated with amino acids for 10 min were stained for mTOR and Lamp2. Scale bars, 20 □m. (**c**) Quantification of mTOR translocation in RagA/B$^{+/+}$ and RagA/B$^{-/-}$ MEFs stably expressing GPR137B or not. Error bars are ± SD of population average and One-way ANOVA analysis followed by Tukey's test shows that there is statistical significance among control groups with or without GPR137B, but not among RagA/B$^{-/-}$ MEFs without or without GPR137B. ; n=5 replicates from 2 independent experiments. In **b** and subsequent figures, *, p=0.01 to 0.05; **, p=0.001 to 0.1, ***, p<0.001. (**d**) Expression of constitutively active RagA/C heterodimer (RagAQ66L/T75N) rescued mTOR translocation in cells treated with siGPR137B. *Left*, HeLa cells transfected with GPR137B siRNA and RagAQ66L/ RagCT75N then stained for mTOR. Cells co-expressing CA RagA/C are marked by blue-dashed lines. *Right*, Analysis of effects on mTOR translocation by Lamp1-GFP or CA RagA/C expression in cells treated with siGPR137B versus siControl. Error bars are ± SD of population average and P value is calculated using two-tailed Student's t test; n=4 independent experiments; Scale bar, 20 □m. (**e**) GPR137B does not induce additional mTOR translocation in Nprl3 null HEK293E cells that have constitutively active RagA. Parental HEK293E cells or Nprl3 KO cells transfected with either Lamp1-Turquoise or GPR137B-Turquoise were treated as in **a**. Error bars represent mean ±SD. P value is calculated using two-tailed Student's t test; n=2 independent experiments.

Figure 4. GPR137B forms an amino acid sensitive complex with mTORC1 through Rag GTPases and

binds RagA constitutively as an adaptor for lysosomal localization.

(**a**) GPR137B interacts with mTOR, Raptor, RagA and Sestrin2, and binding interactions of GPR137B with mTOR and Raptor are amino acid-dependent. HEK293T cells stably expressing Lamp1- or GPR137B-3xFLAG were amino acid-starved for 2 hours and stimulated for 10 min. The cells were chemically cross-linked, lysed and subjected to FLAG immunoprecipitation to detect interactions of GPR137B and putative mTORC1 regulating proteins. (**b**) Rag GTPases are necessary for the GPR137B–mTOR interaction and for an amino acid- regulated recruitment of multiple GPR137B proteins into a lysosomal Rag/mTORC1 signaling complex. GPR137B-3xFLAG and GPR137B-HA were stably expressed in control or RagA/B$^{-/-}$ MEFs. Cells were starved of amino acids and re-stimulated. Cells were then chemically crosslinked and immunoprecipitation was performed using with an anti-FLAG antibody. Co-immunoprecipitated mTOR was detected by Western blot analysis. (**c**) RagA overexpression restores GPR137B self-interaction regardless of RagA GTP status. RagA TN, WT or QL mutants were expressed in RagA/B$^{-/-}$ MEFs. Cells were amino acid starved for 4 hours then stimulated for 20 minutes(**d**) GPR137B can increase mTOR translocation independent of Sestrins. Control (parental HEK293T) cells and Sestrin 1,2,3 triple-null cells transfected with either Lamp1-Turquoise or GPR137B-Turquoise were amino acid-starved for 60 min and re-stimulated for 10 min. GPR137B overexpression still increases mTOR translocation significantly in Sestrin 1,2,3, triple-null HEK293T cells. Error bars represent mean ± SD. (**e**) Amino acid stimulation reduces lysosome localization of RagA and GPR137B increases RagA localization at lysosomes. Increasing expression of GPR137B causes gradual increase in lysosome localization of mTOR, *left*, as well as of RagA, *right*. Amino acid-starved or re-stimulated HeLa cells expressing either Lamp1-Turquoise or GPR137B-Turquoise were stained for endogenous mTOR or RagA and Lamp2, and binned for different levels of Turquiose expression. The median value for each bin is plotted as an average of triplicates ± SD. One-way ANOVA analysis and followed by Tukey's test shows statistically significant differences among different expression bins of GPR137B but not Lamp1. (**f, g**) Knockdown of GPR137B decreases lysosomal localization of RagA in **f** and of RagC in **g** in amino acid-starved and re-stimulated HeLa cells. One-way ANOVA analysis followed by Tukey's test shows statistically significant difference between all siRNA groups and control.

Figure 5: Evidence that GPR137B can activate Rag A/C even in absence of amino acids.

(**a**) mTORC1 interaction with HA-RagA was markedly reduced in cells treated with siGPR137B. GPR137B was knocked down in HEK293T cells stably expressing HA-RagA. HA-RagA was

immunoprecipitated and the interaction with endogenous mTORC1 subunits was detected by Westernblot. (**b**) mTORC1 interaction with HA-RagA was increased in GPR137B overexpressing cells. GPR137B was transiently overexpressed in HEK293T cells stably expressing HA-RagA. In **a** and **b,** the cells were amino acid-starved for 2 hours then treated with starvation or amino acid-containing media for 10 min. Cells were then treated with a cell-permeable chemical cross-linker (DSP) and subjected to HA immunoprecipitation. (**c**) GPR137B knockdown increases HA-RagA-Sestrin2 interaction in amino acid-stimulated cells. HEK293T cells stably expressing HA-RagA were transfected with siGPR137B and co-immunoprecipitation was performed as described above. (**d**) Overexpression of GPR137B reduced Sestrin2 interaction to HA-RagA. GPR137B was over expressed transiently and Sestrin2 interaction to HA-RagA is examined by immunoprecipitation assay. (**e**) Analysis of synergism between GPR137B and Rags for mTORC1 activation. GPR137B co-expression with RagC promotes Rag expression-dependent recruitment of mTORC1 during amino acid starvation (10-12hrs). Control heatmap experiments show co-expression of Lamp1 with RagC does not induce mTORC1 translocation at any expression level of Lamp1 or RagC (*left*), but co-expression of GPR137B with RagC causes synergistic mTORC1 translocation at even low levels of RagC expression in the absence of amino acids. Heatmaps are plotted from translocation scores pooled from 3 independent experiments. (**f**) Synergy analysis as in **e** comparing GPR137B expressing and control Lamp1 expressing cells. Expression dependence of mTORC1 translocation on RagC when co-expressed with Lamp1 or GPR137B during amino acid starvation (10-12hrs) was analyzed. There is a sharp expression dependence of mTORC1 translocation on RagC expression only when co-expressed with GPR137B. Error bars represent mean ± SD and n=3 independent experiments. In **e** and **f**, RagC expression is used as a readout of RagA/C dimer expression. (g) GPR137B co-expression with wildtype Rag A/C promotes RagA/C expression-dependent mTORC1 translocation in RagA/B-/- MEFs in the absence of amino acids, and this effect is significantly reduced in RagA/B-/- MEFs co-expressing GPR137B and dominant negative RagA/C (RagA T21L/RagC Q120L). RagA/B-/- MEFs transiently expressing either Lamp1 as control or GPR137B, along with WT or DN Rag A/C proteins, starved for 2hrs and fixed and stained for mTOR and Lamp2. >20,000 cells analyzed per condition.

Figure 6: Using the kinetics of RagA/C lysosome exchange rate to evaluate the role of GPR137B in regulating Rags

(**a**) Endogenous Rag A/C dissociates from lysosomes upon amino acid stimulation. HeLa cells amino acid-starved for 60 min and re-stimulated for 5 min, were stained for endogenous mTOR, RagA, RagC and Lamp1 as control. Correlation of staining with lysosomal marker Lamp2 is used to measure

lysosomal localization. Error bars represent mean ± SD from 3 independent experiments. P values are calculated from two-tailed Student's t test comparing starved and re-stimulated cells for each antibody. (**b**) Representative images of endogenous mTOR and RagA staining in HeLa cells treated as in **a**. Scale bar, 20 □m. (**c**) Endogenous RagA and RagC dissociate from lysosomes with kinetics anti-correlated with mTOR translocation. HeLa cells amino acid-starved for 60 min and re-stimulated with amino acids for 20s, 120s and 420s were stained as in **a**. (**d**) In the presence of amino acids, rapamycin increases lysosomal retention of mTOR despite accelerating the dissociation of RagA and RagC from lysosomes. HeLa cells amino acid-starved for 60 min were re-stimulated with amino acids in the absence or presence of 20nM rapamycin for 60 min, and stained as in **a**. P values are calculated from two-tailed Student's t test. (**e**) Representative images of endogenous mTOR and RagA staining in HeLa cells treated as in **d**. Scale bar, 20 □m. (**f**) Endogenous RagA dissociates from lysosomes with kinetics anti-correlated with mTOR translocation in the presence of 20 nM rapamycin. HeLa cells amino acid-starved for 60 min and re-stimulated with amino acids for 30s, 90s, 3 min, 30 min and 60 min were stained as in **a**. (**g, h**) Photobleaching recovery measurements of RagC exchange at lysosomes. Lysosome-localized, bleached Venus-RagC exchange faster with unbleached Venus-RagC following photobleaching in cells that co-express constitutively active RagA compared to cells that co-express dominant negative RagA. Images of Hela cells expressing constitutively active RagA (HA GST RagA66L) (*top*) or dominant-negative RagA (HA GST RagA21L) (*bottom*) paired with wildtype Venus-RagC before (frame 1) and after photobleaching (frame 2-4). Red box denotes RagA/C expressing lysosomes that was bleached with a 515 nm laser for 1s. Frames are taken every 10s with a confocal microscope at 40x. Scale bar, 5 □m. Averaged photobleaching recovery curves ± SD for RagA CA (n=6) and RagA DN (n=7) are plotted in **h**. (**i**) Lysosomal Venus-RagC intensity recovers faster in the presence of amino acids than in the absence of amino acids after photobleaching. n=10 each. (**j**) Lysosomal Venus-RagC intensity recovers faster when co-expressed with GPR137B compared to co-expressed with Lamp1 in the absence of amino acids after photobleaching. Lamp1, n=9 and GPR137B, n=7. In **h-j**, error bars represent ± SD of the mean and intensities are normalized to frame immediately before photobleaching. Each n is an individual lysosome from an independent cell. (**k**) Bar graph representation of data in **h-j**. n=3 independent experiments with error bars representing mean ± SD and P values are calculated from two-tailed Student's test. (**l,m**) Lysosomal Venus-RagC intensity recovers slower in cells treated with siGPR137B compared to cells treated with siControl in the presence of amino acids after photobleaching. Lamp1, n=9 and GPR137B, n=9. (**m**) Bar graph representation of data in (**l**) n=3 independent experiments with error bars representing mean ± SD and P values are calculated from two-tailed Student's test.

Figure 7: Rag and Raptor can associate in the cytoplasm

(**a**) Raptor translocates to the plasma membrane along with C1-domain tagged RagC upon addition of phorbol myristate acetate (PMA). Images of HEK293Ts transiently transfected with YFP-Raptor, C1-mRuby-RagC, HA-CA RagA (RagAQ66L), and a plasma membrane CAAX-iRFP marker before and after 3uM PMA. Scale bar 5 μm (**b**) Magnified images of Raptor and C1-RagC translocation to the plasma membrane and line scan profiles measuring the intensities across the plasma membrane edge. White lines indicate positions of the line scan profiles (**c**) Quantification of plasma membrane and cytoplasmic intensity ratio of YFP-Raptor in cells expressing either wildtype RagC or C1-RagC, along with YFP-Raptor, HA-CA RagA and CAAX-iRFP. Only low YFP-Raptor expressing cells are analyzed. n=3 independent experiments with error bars representing mean ± SD and P values are calculated from two-tailed Student's test.

Figure 8: Knockout of human GPR137B reduces lysosomal RagA localization, increases lysosomal compartment and autophagy marker LC3B, and *gpr137b* zebrafish mutants display expanded lysosome compartment in microglia and increased expression of TFEB targets.

(**a, b**) Confocal images of HapI parental, GPR137B KO and GPR137 KO cells stained with Hoechst and LysotrackerGreen (500nm for 60 min). GPR137B KO and GPR137 KO have enlarged lysosomes visualized by LysotrackerGreen. Quantification in **b** and every KO has statistically significant upregulation from parental. (**c**) HapI GPR137 KO and GPR137B KO cells have increased number of autophagosomes and/or autolysosomes as measured by endogenous LC3B puncta in response to amino acid starvation. Every KO has statistically significant upregulation from parental. (**d**) Amino acid-induced mTOR translocation is not statistically significantly different in HapI GPR137B KO and GPR137 KO cells compared to parental cells. (**e**) Lysosomal localization of RagA is reduced in HapI GPR137B KO and GPR137 KO cells. Every KO has statistically significant downregulation from parental in both amino acid-starved and re-stimulated conditions. In **b-e**, n=3 independent experiments with error bars representing the mean ± SD and statistical significance is calculated using One-way ANOVA analysis followed by Tukey's test. (**f, g**) *gpr137ba*$^{-/-}$ and wildtype zebrafish have comparable numbers of neutral red positive microglia. (**h**) Images of LysoTracker Red staining in wildtype (left), and *gpr137ba*$^{-/-}$ zebrafish larvae (right), show enlarged lysosomal compartments in the microglia of *gpr137ba*$^{-/-}$ fish. LysoTracker Red positive compartments are segmented and analyzed for area in wildtype and *gpr137ba*$^{-/-}$ (bottom). **(i)** Quantification of area of LysoTracker Red punctae in zebrafish microglia shows that *gpr137ba*$^{-/-}$ fish have significantly (p=0.0015) larger LysoTracker Red positive compartments. Scale bar, 50 μm. (j) Quantitative real time PCR analysis shows increased relative expression of Transciption Factor EB targets in pooled *gpr137ba*$^{-/-}$ zebrafish relative to a pool of heterozygous (*gpr137ba*$^{+/-}$) controls;

mutations in *gpr137* and *gpr137c* are equally represented in both pools (see text and Methods). Error bars represent standard error of mean. Unpaired, parametric two-tailed T-test with Welch's correction was performed on all samples; * = $p<0.05$, ** = $p<0.01$.

SUPPLEMENTAL FIGURE LEGENDS

Supplementary Figure 1: Additional figure panels describing the primary rpS6 screen and the secondary mTOR translocation screen

(**a**) rpS6 phosphorylation is a robust and sensitive readout for mTORC1 activation using leucine and various known inhibitors of the mTORC1 pathway. Hs68 cells were starved of serum and amino acids for 2.5 hrs and re-stimulated as indicated. Images were quantified by CellProfiler and integrated cytoplasmic intensity of pS6 was used as a measure of mTORC1 activation. (**b**) Screen quality assessed by quantification of siRNA-mediated changes in integrated single cell rpS6 phosphorylation immunofluorescence intensities for all siControl, siRHEB, and siTSC2 wells in the primary screen (n=384 each). Each point represents the average of triplicates for the same well position, normalized by the plate median and the plate standard deviation. (**c**) *Left*, The strongest single siRNA effect in each pool of siRNAs dominates the pool behavior in the primary screen. The value of the strongest single siRNA effect is plotted on the X-axis against the primary screen value on the Y-axis. *Right*, the rpS6 phosphorylation effect of the average of the second and third strongest single siRNA effects is plotted on the X-axis against the primary screen Z-score on the Y-axis. This provides an independent validation that the effect of the siRNA knockdown is specific. (**d**) Pathway analysis (Ingenuity) shows statistical enrichment and number of deconvolution hits in a subset of canonical pathways (red and green for negative and positive regulators, respectively). Only siRNAs selected as unbiased top hits were used in analysis. P-values were calculated by the right-tailed Fisher's exact test. (**e**) Image-based correlation

analysis shows cycloheximide stimulated and RagC-dependent colocalization of mTORC1 and Lamp2. Error bars are ± SD of population average; n=6 wells from 4 independent experiments.

Supplementary Figure 2: Validation of GPR137B as a regulator of amino acid-induced mTORC1 translocation to lysosomes

(**a**) Two independent synthetic siRNAs targeting GPR137B efficiently knockdown GPR137B mRNA levels as measured by qPCR. Error bars are ± SD of population averages; n= 6 from 3 independent experiments. (**b**) Knockdown of GPR137B in HeLa cells reduces amino acid-stimulated mTOR translocation. Error bars are ± SD of population average; n=6 to 8 wells from 3 independent experiments. (**c**) Rescue of mTOR translocation by GPR137B-Turquoise expression in HeLa cells treated with 3'UTR GPR137B siRNA. Error bars ± SEM of the population average; n=6 wells from 2 independent experiments. (**d**) Cells treated with siGPR137B reduces phosphorylation of rpS6 at 240/244 in resting state and 120min after amino-acid stimulation. Level of rpS6 phosphorylation at 240/244 was quantified in Hs68 cells treated with siRNAs against Control, GPR137B and RRAGC. 68-72hrs post transfection, cells were amino-acid starved and re-stimulated with amino acids for indicated time points or left in resting media. n=3 independent experiments with error bars representing mean ± SD, n>1,000 cells per well, and One-way ANOVA analysis followed by Tukey's test was used. **(e)**The GPR137B-Turquoise mediated increase in mTORC1 translocation is not a result of a change in lysosome size as indicated by amount of Lamp2 staining. Error bars ± SEM of the population average; P values were calculated in comparison to untransfected cells in the same well; n>500 cells each condition; scale bar 20 □m. (**f**) Expression of GPR137 and GPR137C mediates an increase in mTOR recruitment in amino acid-starved cells. HeLa cells were transfected with GPR137-YFP or GPR137C-YFP, then starved of amino acids and serum for 4 hrs, followed by fixation and staining with antibodies against GFP and mTOR. Red * indicates transfected cells. Scale bars, 10 □m. (**g**) Quantification of **f**. (**h**) Control experiment showing that Lamp1-GFP overexpression does not increase the amino-acid sensitive and Torin-sensitive 4E-BP1 phosphorylation at residues 36/47. Error bars ± SEM of the population average. (**i,j**) Lack of rescue of mTOR translocation and activity by GPR137B in serum-starved cells. (**i**) Amount of mTOR localized at the lysosomes was quantified in Hs68 cells transiently-transfected with either control lysosomal protein, Lamp1 or GPR137B and serum-starved overnight, or amino-acid starved for 3hrs in presence of dialyzed FBS. Starved cells were re-stimulated with serum for 30min or amino acids for 10min respectively. Fold induction of mTOR translocation over Lamp1 control was compared for GPR137B expressing cells and untransfected cells in the same well. (**j**) Levels of phosphorylated p4EBP1 37/46 was quantified in cells treated as in (**i**) and re-stimulated with serum or amino acids for 30min. For (**i** and **j**) n=4 and 3

independent experiments with error bars representing mean ± SD, n>1,000 cells per well, and Student's test is used.

Supplementary Figure 3. Rag GTPase-dependent mTORC1 translocation and GPR137B-mTOR interaction

(**a**) Representative images show mTOR translocation is abolished in RagA/B$^{-/-}$ MEFs. Scale bars, 20 □m. (**b**) Rag GTPases are required for interaction of mTOR and GPR137B. mTOR and GPR137B -3xFLAG co-immunoprecipitation was examined in RagA/B knockout MEFs stably expressing GPR137B -3xFLAG.

Supplementary Figure 4: Additional experiments evaluating GPR137B interactions and GPR137B as an adaptor of lysosomal Rag A/C.

(**a**) Immunoprecipitation of FLAG-NPC1 from lysates of HEK293T cells stably expressing FLAG-tagged NPC1 did not co-immunoprecipitate mTORC1 components or Rag GTPases. Cells are treated as in Figure 4A. (**b**) Interaction of GPR137B with mTORC1 and RagA were investigated in HeLa cells stably expressing GPR137B -3xFLAG. (**c**) GPR137B does not interact with SLC38A9. Co-immunoprecipitation was performed as Figure 4A. (**d**) **Quantification of Figure 4c.** (**e**) GPR137B regulates RagC lysosome localization. Increasing expression of GPR137B causes increased lysosomal RagC localization. Amino acids-starved or re-stimulated HeLa cells expressing either Lamp1-Turquoise or GPR137B-Turquoise were stained for endogenous RagC and Lamp2, and binned for different levels of Turquiose expression. The median value for each bin is plotted as an average of triplicates ± SD. GPR137B expressing bins show statistically-significant differences with $p<0.005$ by One-way ANOVA analysis and p values from Tukey's test are plotted for specific intergroup comparisons. *, p=0.01 to 0.05; **, p=0.001 to 0.1, ***, $p<0.001$ (**f, g**) Lack of Rescue of RagA localization and mTORC1 activity by GPR137B expression in siRagulator treated cells. (**f**) Amount of RagA localized at the lysosomes was quantified in HeLa cells transiently-transfected with the indicated siRNA and cDNAs, amino acid-starved for 2hrs and re-stimulated for 10min. All values are normalized to control cells (siControl treated expressing Lamp1). One-way ANOVA analysis followed by Tukey's test show statistically-significant

difference among all groups except between Lamp1-expressing and GPR137B-expressing cells in siLamtor3 treated wells, in both amino acid-starved and re-stimulated conditions. (**g**) Levels of phosphorylated p4EBP1 37/46 was quantified in cells treated as in (A) and re-stimulated with amino acids for 30min. In wells treated with siLamtor3, Student's paired t-test shows no statistically-significant difference between GPR137B-expressing cells and the untransfected cells of the same well. (A and B) n=4-6 wells from 2 independent experiments with error bars representing mean ± SD, n>1,000 cells per well.

Supplementary Figure 5. Repeat and quantification of Figure 5 western blots

(**a**) GPR137B knockdown decreases mTORC1-RagA and increases RagA-Sestrin2 interactions in amino acid stimulated cells. HEK293T cell stably expressing HA-RagA was transfected with siGPR137B. HA-RagA was immunoprecipitated and mTOR, raptor, and Sestrin2 interaction was examined. (**b**) Quantification of (**a**) N=3. (**c**) Overexpression of GPR137B increases mTORC1 and reduces Sestrin2 interactions to RagA. GPR137B-FLAG was overexpressed in HA-RagA expressing HEK293T cells and HA immunoprecipitation was performed. (**d**) Quantification of (**c**) N=3.

Supplementary Figure 6. GPR137B as an activator of lysosomal RagA/C

(**a**) GPR137B co-expression with RagA/C enables RagA/C expression-dependent recruitment of mTORC1 under amino acid starvation (2hrs). Heatmaps show co-expression of GPR137B-mCherry with Rap2A does not induce Rap2A expression-dependent recruitment of mTORC1 translocation, *left*, but co-expression of GPR137B with RagA/C causes mTORC1 translocation at low levels of RagA/C expression, *right*. HeLa cells were amino acid-starved for 2hrs in dialyzed serum, and cells co-expressing GPR137B-mCherry and Rap2A-CFP (n=958) or GPR137B-mCherry and RagA/C-CFP (n=1466) were binned into 8 equal bins of CFP intensities and mCherry intensities. Average of mTOR translocation score for each bin is plotted as a blue-yellow heatmap scaled from 50-450. Gray indicates bins where there was insufficient number of cells. Heatmaps are plotted from translocation scores pooled from 2 independent experiments. (**b**) Calibration of wildtype RagC-Turquoise (paired with HA-tagged wildtype RagA) and Q120L RagC-CFP (paired with HA-tagged dominant negative RagA) fluorescence intensity using an endogenous RagA antibody. To correct for fluorophore differences between Turquoise and CFP for the heatmap in Fig. 5e, we measured the RagC fluorescence intensity and RagA antibody stain intensity in the same cell and plotted the average of the RagA intensity for each bin of RagC fluorescence intensity to correlate RagA protein levels to RagC fluorescence intensities. We then normalized RagC-DN intensity values by the

ratio of the correlation slopes to adjust them to reflect the same amount of RagA proteins at the same wildtype RagC intensities. (**c**) Histograms of measurements for expression level of Lamp1, expression level of GPR137B and level of mTOR translocation, for all cells in the heatmap experiment in Fig. 5e. Red bracket in each histogram shows most of the values for each parameter is included in the heatmap and therefore represent the population accurately. (**d**) Repeat of experiment in Fig. 5e demonstrating synergistic activation of mTORC1 by GPR137B and wildtype RagA/C, and reduced effect by GPR137B and dominant negative RagA/C in RagA/B-/- MEFs in the absence of amino acids. n>20,0000 cells analyzed per condition. (**e,f**) Lysosomal Venus-RagC intensity recovers similarly when co-expressed with GPR137B or with Lamp1 in Nprl3-/- HEK293E cells in the absence of amino acids after photobleaching. Lamp1, n=9 and GPR137B, n=9. (**f**) Bar graph representation of data in **e**. n=3 independent experiments with error bars representing mean ± SD and P values are calculated from two-tailed Student's test.

Supplementary Figure 7. Validation of C1 domain-tagged RagC constructs in pulling RagA heterodimer and Raptor to the plasma membrane.

(**a**) C1-domain tagged RagC can pull wildtype RagA to the plasma membrane. Two C1-domains fused to N-terminus of RagC (C12x-RagC) co-expressed with wildtype RagA in HapI cells were stimulated with 1□M PMA and fixed. Scale bars, 10 □m (**b**) C12x-RagC mediated Raptor recruitment to plasma membrane unlikely involves lysosomes being pulled to the plasma membrane. HEK293Ts co-expressing C12xRagC anad YFP-Raptor were treated with 1□M PMA, fixed and stained for Lamp2. C12x-RagC co-localization with Raptor, C12xRagC co-localization with endogenous Lamp2, and Raptor co-localization with Lamp2 are shown in the bottom panel. Scale bars, 10 □m (**c**) Examples of dim Raptor expressing cells analyzed in Fig. 7c show translocation of both Raptor and C1-RagC to the plasma membrane. Top panel shows frame before 3□M PMA addition and table shows background intensity and average cell intensity for Raptor and RagC channels. C1-RagC was used instead of C12X-RagC to reduce the basal plasma membrane of both RagC and Raptor pre-drug addition due to lower phorbal-ester binding affinity. Scale bars, 20 □m.

Supplementary Figure 8. Results of knockouts of GPR137B and of its isoform GPR137 in human cells and of gpr137b knockout in zebrafish

(**a**) Relative fold change of mTOR translocation in response to amino acids is not reduced in HapI

GPR137B KO and GPR137 KO cells compared to parental control. One-way ANOVA analysis followed by Tukey's test shows that no KO group has statistically significant down-regulation of amino acid sensitive mTOR translocation. (**b**) Table showing percentage amino acid sequence identity between zebrafish gpr137 homologs and human GPR137B; gpr137ba shows the highest sequence similarity to the human GPR137B homolog. **(c)** Amino acid alignment of zebrafish gpr137ba and human GPR137B showing a high degree of conservation between the two sequences. (d) Sequence validation of *gpr137ba* zebrafish generated by TALEN. (**e**) Wildtype and *gpr137ba* mutant zebrafish are viable, images represent whole fish mounts of the indicated genotypes at 5 dpf. Scale bar, 50 μm. (**f**) Immunoblot on whole zebrafish tissue shows that *gpr137ba*$^{-/-}$ zebrafish do not have increased LC3B or p62, or reduced phosphorylation of S6. (**g**) Presence and absence of homologs of GPR137, mTOR, Rags and Ragulator in 179 eukaryotic speciesAnalyzed eukaryotic species (179) that have, or do not have, homologs of human GPR137B using an algorithm described in (Dey et al., 2015). A hand-drawn illustrative human-centric species tree is shown where species are highlighted that have GPR137B homologs. GPR137B homologs are present in all vertebrates examined and in many invertebrates as well as in eukaryotic species as divergent as *Dictyostelium discoideum* and *Monosiga brevicollis*, but not in more ancestral plants and protists. GPR137B homologs are also not found in fungi, *C.elegans*, and Drosophila model systems.

SUPPLEMENTAL TABLES

Supplementary Table 1:

Excel spreadsheet with all 21,041 human siRNA pools tested in the genome-wide screen. Three added columns indicate whether (1) a gene was selected for deconvolution (testing each of the 4 individual siRNAs in a pool); (2) a gene with a phospho-rpS6 phenotype that was confirmed by more than three siRNAs and (3) a gene with a phospho-rpS6 phenotype that passed the selection criterion of having strongest siRNA as well as the average of the second and third strongest siRNA effect being significant hits.

Supplementary Table 2:

List of canonical pathways identified by Ingenuity Pathway Analysis of validated siRNAs associated, shown in Supplemental Figure 1D.

REFERENCES

1. Hirose, E., Nakashima, N., Sekiguchi, T. & Nishimoto, T. RagA is a functional homologue of S. cerevisiae Gtr1p involved in the Ran/Gsp1-GTPase pathway. *J. Cell Sci.* **111,** 11–21 (1998).
2. Schürmann, A., Brauers, A., Massmann, S., Becker, W. & Joost, H. G. Cloning of a novel family of mammalian GTP-binding proteins (RagA, RagBs, RagB1) with remote similarity to the Ras-related GTPases. *J. Biol. Chem.* **270,** 28982–8 (1995).
3. Sekiguchi, T., Hirose, E., Nakashima, N., Ii, M. & Nishimoto, T. Novel G proteins, Rag C and Rag D, interact with GTP-binding proteins, Rag A and Rag B. *J. Biol. Chem.* **276,** 7246–57 (2001).
4. Sancak, Y. *et al.* The Rag GTPases bind raptor and mediate amino acid signaling to mTORC1. *Science* **320,** 1496–501 (2008).
5. Kim, E., Goraksha-Hicks, P., Li, L., Neufeld, T. P. & Guan, K.-L. Regulation of TORC1 by Rag GTPases in nutrient response. *Nat. Cell Biol.* **10,** 935–945 (2008).
6. Sancak, Y. *et al.* Ragulator-rag complex targets mTORC1 to the lysosomal surface and is necessary for its activation by amino acids. *Cell* **141,** 290–303 (2010).
7. Bar-Peled, L., Schweitzer, L. D., Zoncu, R. & Sabatini, D. M. Ragulator Is a GEF for the Rag GTPases that Signal Amino Acid Levels to mTORC1. *Cell* **150,** 1196–1208 (2012).
8. Bar-Peled, L. *et al.* A Tumor suppressor complex with GAP activity for the Rag GTPases that signal amino acid sufficiency to mTORC1. *Science* **340,** 1100–6 (2013).
9. Panchaud, N., Péli-Gulli, M.-P. & De Virgilio, C. Amino acid deprivation inhibits TORC1 through a GTPase-activating protein complex for the Rag family GTPase Gtr1. *Sci. Signal.* **6,** ra42 (2013).
10. Efeyan, A. *et al.* Regulation of mTORC1 by the Rag GTPases is necessary for neonatal autophagy and survival. *Nature* **493,** 679–83 (2013).
11. Ricoult, S. J. H. & Manning, B. D. The multifaceted role of mTORC1 in the control of lipid metabolism. *EMBO Rep.* **14,** 242–251 (2012).
12. Huang, J. & Manning, B. D. A complex interplay between Akt, TSC2 and the two mTOR complexes. *Biochem. Soc. Trans.* **37,** 217–22 (2009).

13. Inoki, K., Zhu, T. & Guan, K.-L. TSC2 Mediates Cellular Energy Response to Control Cell Growth and Survival. *Cell* **115,** 577–590 (2003).

14. Potter, C. J., Pedraza, L. G. & Xu, T. Akt regulates growth by directly phosphorylating Tsc2. *Nat. Cell Biol.* **4,** 658–665 (2002).

15. Linares, J. F. *et al.* K63 Polyubiquitination and Activation of mTOR by the p62-TRAF6 Complex in Nutrient-Activated Cells. *Mol. Cell* **51,** 283–296 (2013).

16. Rebsamen, M. *et al.* SLC38A9 is a component of the lysosomal amino acid sensing machinery that controls mTORC1. *Nature* **519,** 477–481 (2015).

17. Wang, S. *et al.* Metabolism. Lysosomal amino acid transporter SLC38A9 signals arginine sufficiency to mTORC1. *Science* **347,** 188–94 (2015).

18. Jung, J., Genau, H. M. & Behrends, C. Amino Acid-Dependent mTORC1 Regulation by the Lysosomal Membrane Protein SLC38A9. *Mol. Cell. Biol.* **35,** 2479–2494 (2015).

19. Kim, Y. C. *et al.* Rag GTPases are cardioprotective by regulating lysosomal function. *Nat. Commun.* **5,** 4241 (2014).

20. Averous, J. *et al.* Requirement for lysosomal localization of mTOR for its activation differs between leucine and other amino acids. *Cell. Signal.* **26,** 1918–1927 (2014).

21. Shen, K., Sidik, H. & Talbot, W. S. The Rag-Ragulator Complex Regulates Lysosome Function and Phagocytic Flux in Microglia. *Cell Rep.* **14,** 547–559 (2016).

22. Cai, W., Wei, Y., Jarnik, M., Reich, J. & Lilly, M. A. The GATOR2 Component Wdr24 Regulates TORC1 Activity and Lysosome Function. *PLoS Genet.* **12,** e1006036 (2016).

23. Soma-Nagae, T. *et al.* The lysosomal signaling anchor p18/LAMTOR1 controls epidermal development by regulating lysosome-mediated catabolic processes. *J. Cell Sci.* **126,** 3575–84 (2013).

24. Ruvinsky, I. & Meyuhas, O. Ribosomal protein S6 phosphorylation: from protein synthesis to cell size. *Trends Biochem. Sci.* **31,** 342–348 (2006).

25. Rosner, M. & Hengstschläger, M. Evidence for cell cycle-dependent, rapamycin-resistant phosphorylation of ribosomal protein S6 at S240/244. *Amino Acids* **39,** 1487–92 (2010).

26. Beugnet, A., Tee, A. R., Taylor, P. M. & Proud, C. G. Regulation of targets of mTOR (mammalian target of rapamycin) signalling by intracellular amino acid availability. *Biochem. J.* **372,** 555–66 (2003).

27. Gao, J. *et al.* TM7SF1 (GPR137B): a novel lysosome integral membrane protein. *Mol. Biol. Rep.* **39,** 8883–9 (2012).

28. Chan, E. Y. mTORC1 Phosphorylates the ULK1-mAtg13-FIP200 Autophagy Regulatory Complex. *Sci. Signal.* **2,** pe51-pe51 (2009).

29. Gingras, A.-C., Raught, B. & Sonenberg, N. Regulation of translation initiation by FRAP/mTOR. *Genes Dev.* **15,** 807–826 (2001).

30. Miron, M., Lasko, P. & Sonenberg, N. Signaling from Akt to FRAP/TOR targets both 4E-

BP and S6K in Drosophila melanogaster. *Mol. Cell. Biol.* **23,** 9117–26 (2003).

31. Fingar, D. C., Salama, S., Tsou, C., Harlow, E. & Blenis, J. Mammalian cell size is controlled by mTOR and its downstream targets S6K1 and 4EBP1/eIF4E. *Genes Dev.* **16,** 1472–87 (2002).

32. Chantranupong, L. *et al.* The Sestrins Interact with GATOR2 to Negatively Regulate the Amino-Acid-Sensing Pathway Upstream of mTORC1. *Cell Rep.* **9,** 1–8 (2014).

33. Kim, J. S. *et al.* Sestrin2 inhibits mTORC1 through modulation of GATOR complexes. *Sci. Rep.* **5,** 9502 (2015).

34. Wolfson, R. L. *et al.* Sestrin2 is a leucine sensor for the mTORC1 pathway. *Science (80-.).* **351,** 43–48 (2016).

35. Parmigiani, A. *et al.* Sestrins Inhibit mTORC1 Kinase Activation through the GATOR Complex. *Cell Rep.* **9,** 1281–1291 (2014).

36. Peng, M., Yin, N. & Li, M. O. Sestrins function as guanine nucleotide dissociation inhibitors for Rag GTPases to control mTORC1 signaling. *Cell* **159,** 122–133 (2014).

37. Oshiro, N., Rapley, J. & Avruch, J. Amino acids activate mammalian target of rapamycin (mTOR) complex 1 without changing Rag GTPase guanyl nucleotide charging. *J. Biol. Chem.* **289,** 2658–74 (2014).

38. Deng, L. *et al.* The ubiquitination of rag A GTPase by RNF152 negatively regulates mTORC1 activation. *Mol. Cell* **58,** 804–18 (2015).

39. Jin, G. *et al.* Skp2-Mediated RagA Ubiquitination Elicits a Negative Feedback to Prevent Amino-Acid-Dependent mTORC1 Hyperactivation by Recruiting GATOR1. *Mol. Cell* **58,** 989–1000 (2015).

40. Zhou, X. *et al.* Dynamic Visualization of mTORC1 Activity in Living Cells. *Cell Rep.* **10,** 1767–1777 (2015).

41. Manifava, M. *et al.* Dynamics of mTORC1 activation in response to amino acids. *Elife* **5,** (2016).

42. Xie, J., Wang, X. & Proud, C. G. mTOR inhibitors in cancer therapy. *F1000Research* (2016). doi:10.12688/f1000research.9207.1

43. Dey, G., Jaimovich, A., Collins, S. R., Seki, A. & Meyer, T. Systematic Discovery of Human Gene Function and Principles of Modular Organization through Phylogenetic Profiling. *Cell Rep.* **10,** 993–1006 (2015).

44. Efeyan, A. *et al.* RagA, but Not RagB, Is Essential for Embryonic Development and Adult Mice. *Dev. Cell* **29,** 321–329 (2014).

45. Wang, C., Liang, Q., Chen, G., Jing, J. & Wang, S. Inhibition of *GPR137* suppresses proliferation of medulloblastoma cells *in vitro*. *Biotechnol. Appl. Biochem.* **62,** 868–873 (2015).

46. Cui, X. *et al.* Knockdown of *GPR137* by RNAi inhibits pancreatic cancer cell growth and

induces apoptosis. *Biotechnol. Appl. Biochem.* **62,** 861–867 (2015).

47. Andrade, V. P. *et al.* Gene expression profiling of lobular carcinoma in situ reveals candidate precursor genes for invasion. *Mol. Oncol.* (2015). doi:10.1016/j.molonc.2014.12.005

48. Brunetti, M. *et al.* Recurrent fusion transcripts in squamous cell carcinomas of the vulva. *Oncotarget* **8,** 16843–16850 (2017).

50. Bjorkoy, G. *et al*. (2005) p62/SQSTM1 forms proteinaggregates degraded by autophagy and has a protective effect on huntingtin-induced cell death. J Cell Biol 171: 603–614 (2005).

51. Lawrence, RE. *et al*. A nutrient-induced affinity switch controls mTORC1 activation by its Rag GTPase-Ragulator lysosomal scaffold. Nat Cell Biol. Sep;20(9):1052-1063 (2018).

52. Shen, K. *et al*. CaMKIIbeta functions as an F-actin targeting module that localizes CaMKIIalpha/beta heterooligomers to dendritic spines. Neuron. 1998 Sep;21(3):593-606.

Materials and Methods

Cell Lines

HS68 primary fibroblast, HeLa, and HEK293T cells were obtained from ATCC. CRISPR-Cas9 edited HapI cells were purchased from Horizon Discovery. RagA/B knockout and parental MEFs were kindly provided by Dr. Kun-Liang Guan's lab. sgNprl3 and parental HEK293E cells, sgSestrin1/2/3 and parental HEK293T cells were kindly provided by Dr. David Sabatini's lab.

Immunofluorescence

Cells were fixed in 4% formaldehyde in PBS for 30 minutes at RT, washed with PBS followed by 15 minutes of 0.2% Triton X-100 permeabilization on ice. 3% BSA in 1xPBS was used for blocking 30 minutes at RT. Primary antibodies were added overnight at 4°C (Hoechst and fluorescent secondary antibodies were added post washing for 1 to 2 hrs at RT). Images were taken either with a 20X air objective, an automated inverted epifluorescence microscope (ImageXpress 5000A or ImageXpressMicro, Molecular Devices), with a 40X or 60X oil objective on a confocal microscope (Leica TCS SP2 AOBS or 3i imaging system).

Cell Lysis and Immunoprecipitation

0.5-million HEK293T cells stably expressing FLAG-tagged proteins were plated on collagen-coated 10 cm dish. Next day, cells were lysed in 1% Triton X-100 lysis buffer (1% Triton X-100, 50 mM HEPES [pH 7.4], 150 mM NaCl, and protease inhibitor cocktail (Thermo Fisher Scientific) then sonicated briefly at 4˚C. The sample was incubated at 4˚C for 1 hour. After spun at top speed for 30 min, FLAG immuinoprecipitation was performed. See Supplemental Experimental Procedures for more detailed description.

Zebrafish Lines and Maintenance

All work with zebrafish was conducted with approval from the Stanford University Institutional Animal Care and Use Committee. Embryos and larvae were treated with 0.003% 1-phenyl-2-thiourea (PTU) to inhibit pigmentation, and anesthetized with 0.016% (w/v) Tricaine prior to experimental procedures.

Genome-wide siRNA screen and hit selection

The primary screen was performed using human primary foreskin fibroblasts (HS68 cells). Serum was removed to maximize the amino-acid-induced signal. Cells were stimulated after amino acid removal with a 1 x mixture of all amino acids without glutamine (Figure 1B, schematic). An siARRAY whole human genome siRNA library from ThermoFisher Scientific (Formerly Dharmacon, Cat#G-005000-025), containing 21,041 siRNA pools in 267 X 96-well plates, 80 siRNA pools/plate, was screened using a 384 well formatted assay. Three replicates of each mother siRNA plate were tested at 10 nM concentration in the primary screen; a total of 204 384-well plates. All transfections were done using a Vprep (Velocity 11) with a 96 tip disposable tip head. Lipofectamine 2000 addition and cell addition were done with a Wellmate Dispenser (Matrix). All washing steps, including serum-starvation and amino acid starvation were done using the Plate Washer (Bio-TEK). Hs68 cells were reverse-transfected and the transfection mix was removed 18 hrs to 24 hrs later. Cells were then serum-starved with DMEM/0.1% BSA to keep cell numbers consistent among wells. 68 to 72 hours post transfection, cells were amino acid starved in 1.5% BSA/DPBS for 3 hours and re-stimulated with an amino acid mixture (1xAA) prepared from diluting 50X Essential amino acids and 100X non-essential amino acids in 1.5% BSA/DPBS. Cells were fixed and stained with an antibody against rpS6 phosphorylated at 240/244. Phosphorylation of rpS6 was imaged with an automated microscope (Axon, Molecular Devices) and integrated fluorescence intensity was quantified using CellProfiler (Carpenter et al., 2006).

Primary screen analysis

Using automated fluorescence imaging and automated analysis of antibody staining, we averaged the integrated single-cell rpS6 intensities across all cells in a single well. The mean rpS6 phosphorylation intensity for each well was calculated as the deviation from the median of the surrounding 20 wells in the 384-well plate, in order to minimize regional plate artifacts. The

standard deviations of the three replicates of each siRNA treatment (each plate was assayed in parallel in triplicate) were used as a measure of experimental variability (Galvez et al., 2007; Paulsen et al., 2009). The region-corrected means were normalized to the average of the triplicate standard deviations for the entire plate to generate a Z-score = (X-mu)/sigma. The parameter mu was estimated using regional median and the sigma parameters using replicates in each triplicate set. A comparison to nearby 20 wells was used since the library is not randomly organized. Z-scores were normalized to the median Z-score of positive controls (siRheb or siTSC2 controls) in each triplicate set. The resulting fold-change values were used to create a rank-ordered list of genes, and the top 750 genes were selected as hits. An additional list of hits (with a minimum Z-score of 2) was selected based on an additional criterion of matching functional identifiers or literature data (for example: kinase, exchange factor). With these added hits, a total of 1231 genes were selected for further analysis.

Deconvolution of siRNA pools

Using the same assay as in the primary screen, each single siRNA of the 1231 selected pools was tested separately again in a 384-well formatted assay (4 siRNAs targeting the same gene in each pool). Each siRNA was transfected at 10 nM concentration. A quadrant of each plate was filled with siRNA targeting a scrambled sequence (negative controls). The mean integrated rpS6 intensity for each well was region-corrected by subtracting the average of the mean rpS6 intensities of the negative controls in a 22-well neighborhood, and then divided by the standard deviations of the mean rpS6 intensities of all the negative control wells on the same plate. The generated Z-scores were then averaged across duplicates. For each of the original 1231 pools, the deconvolution score was calculated as the average of the 2nd and 3rd strongest single siRNAs. We averaged the 2nd and 3rd strongest siRNA since we noticed a tight correlation between the 1st siRNA and the primary screen pool value (Figure S1C, left), which argued that the strongest siRNA largely recapitulates the screen phenotype. This also means that the averaged 2nd and 3rd hit can provide a second independent test for off-target effects (Figure S1C, right). The resulting rank-ordered list of deconvolution scores was at the end manually pruned (removing high-scoring genes with functions likely unrelated or indirectly related to mTOR signaling, such as secreted or extracellular proteins and adding a few lower-scoring genes with relevant

functional characteristics) to generate a total of 427 deconvolution hits that we further investigated.

mTOR translocation screen

The 427 hits were then assayed for their effect on mTOR translocation. The single siRNA with the strongest pS6 phenotype for each hit (see deconvolution assay above) was tested in duplicate in 96-well format at a concentration of 5 nM and assayed in parallel on a single plate for phospho-S6. Cells were reverse-transfected using the same conditions as the primary screen except both the transfection and the assay were performed manually using multichannel pipettes. Cells were starved of amino acids for 4 hours in 1.5% BSA/DPBS and re-stimulated with cycloheximidefor 5 minutes (mTOR translocation) or 30 minutes (rpS6 phosphorylation). The plates were fixed and stained with antibodies against mTOR and Lamp2 or phospho-S6 (240/244). The correlation coefficient between the intensity of segmented puncta in the mTOR and Lamp2 channels was calculated for each well (see section on puncta analysis) and averaged across duplicates. A Z-score for mTOR translocation was generated by subtracting the plate median and normalizing the result by the plate standard deviation. A Z-score for the parallel phospho-S6 experiment was generated by subtracting the mean of the negative control wells (scrambled siRNA) and normalizing the result to their standard deviation. The plate median was not used in this case because all the genes were expected to perturb rpS6 levels to some extent, having been selected as deconvolution hits in the first place. Hits with a translocation Z-score below -1.8 and rpS6 phosphorylation below -1.6 were considered for further analysis.

Bioinformatics

Ingenuity Systems pathway analysis (www.ingenuity.com) was used to identify enriched pathways and draw networks. The subset of hits solely chosen based on rank selection were uploaded into Ingenuity pathway analysis and the most enriched canonical pathways/diseases were identified. Fisher's exact test was used to calculate a p-value.

Cell Culture and Reagents

HS68 primary fibroblast, HeLa, and HEK293T cells were cultured in 10% FBS/DMEM/PSG (Gibco) medium. HapI parental and knockout cells generated by CRISPR-Cas9 were purchased from Horizon Discovery and cultured in 10% FBS/IMDM. Lipofectamine 2000, DPBS media

used for starvation, 50X Essential amino acids and 100X non-essential amino acids were obtained from Life Technologies. BSA, cycloheximide, and Phorbol 12-myristate 13-acetate (PMA) were from Sigma-Aldrich. Triton X-100 was from Sigma and 16% formaldehyde was from Ted Pella. n-Octyl-β-D-Glucopyranoside was from Affymetrix. GeneSilencer (Genlantis) was used for siRNA and plasmid co-transfection in HeLa cells. Fugene 6 and X-tremeGENE HP (Roche Applied Science) were used for plasmid transfection into HeLa and HEK293T cells. Lipofectamine 2000 was used to transfect DNA or siRNA into HS68, and HEK293T cells. MEF2 Nucleofector kit was purchased from LONZA to electroporate MEFs using the Amaxa Nucleofector. Rapamycin was purchased from Calbiochem. Torin was purchased from Tocris. Amino acid starvation medium (DMEM without amino acids) was purchased from Athena Enzyme Systems. DMEM culture media were used as amino acid add-back medium. Amino acid starvation experiments in screen and FRAP experiments was conducted in 1.5% BSA/DPBS and re-stimulated with an amino acid mixture (1xAA) added to the starvation media. DMEM without amino acids and 10% dialyzed FBS was used as starvation media for all other experiments.

a. GPR137B reagents and various mTORC1 reagents

siRNAs against GPR137B were purchased from Dharmacon as 4 separate duplexes. The sequence with the strongest effect was GGACUAAAGUAUUCCACAA (3'UTR); the second strongest was GCAAUAAUGUAGACUGAUA (3'UTR). siRNAs against LAMTOR2 and LAMTOR3 were purchased from Dharmacon as siGenome Smartpools. cDNAs encoding GPR137 (NM_001170880) and GPR137C (NM_001099652) were purchased from Open Biosystems, now part of GE Healthcare. GPR137B cDNA was obtained from in house human ORFeome collection. All GPR137, B and C fluorescently-tagged proteins were cloned by recombining the cDNA into Gateway destination vectors. Wildtype Venus-RagC, Turquoise-RagC, and Venus-RagA were generated by cloning human ORFeome cDNA into Gateway destination vector. The LC3-GFP (Plasmid #24920), Rat Lamp1-mRFP-2xFLAG (Plasmid #34611) and YPF-Raptor (Plasmid #73385) were obtained from Addgene. Lamp1-Turquoise was subcloned from Rat Lamp1-mRFP-2xFLAG using Gateway destination vectors. pRK5-HA GST RagA 66L(Addgene plasmid # 19300) and pRK5-HA GST RagA 21L(Addgene plasmid # 19299) were gifts from Dr. David Sabatini. YFP-RagC T75N and CFP-RagC Q120L were gifts from Dr. Won Do Heo. NPC1-YFP-2xFLAG was a gift from Dr. Manny Lopez. GPR137B-

3xFLAG and Rat Lamp1-3xFLAG were subcloned into pPBbsr2-IRES-Blasticidin and GPR137B-HA was subcloned into pLV-EF1a-IRES Puromycin vector using Gibson assembly (New England Biolabs). C12x-mRuby-RagC and C1-mRuby-RagC were generated from Gibson assembly using C12x-YFP, C1-YFP and mRuby-T-Plastin which were made by Dr. Damien Garbett. HEK293T cells stably expressing GPR137B-3xFLAG and Lamp1-3xFLAG were generated using PiggyBac transposon system (System Biosciences). GPR137B-HA stable cell-line was generated by lentivirus infection. Positive clones were selected using indicated antibiotics.

b. Antibodies and dyes

Antibodies were obtained from the following sources: anti- pS6 240/244 (IF 1:500), mTOR (IF 1:200 , WB 1:1000), Rictor (WB 1:1000), Raptor (WB 1: 500), Rag C polyclonal (IF 1:200) Rag C monoclonal (IF 1:200, WB 1:250), Rag A (IF 1:200, WB 1:1000), LC3B (IF 1:200), Rheb (WB 1:100), Rheb (WB 1:250) from Cell Signaling Technology; Antibody to the HA tag (3F10) from Roche (IF 1:200 , WB 1:1000); mouse and rabbit antibodies to FLAG epitope (IF 1:300 , WB 1: 1000), FLAG-M2 affinity gel and anti-HA agarose antibody from Sigma Aldrich; antibodies to Lamp1 (IF 1:300 , WB 1:2000), Lamp 2 (IF 1:300), LRS (WB 1:500), FNIP1 (WB 1:1000), p62 (1:300) and GFP (IF 1:500) from Abcam; anti-ATP6V1A (WB 1µg/mL) from GeneTex; NPRL3 (WB 1:500) from Atlas antibodies; Alexa secondary antibodies from Life Technologies; HRP-labeled anti-mouse, anti-rabbit and anti-rat secondary antibodies from Jackson ImmunoResearch. LysotrackerGreen and LysotrackerRed were purchased from ThermoFisherScientific. Mouse anti-HA (Cat#88837 Lot#QJ224632) from Pierce.

Image Analysis and live-cell imaging

a. Analysis of lysosome localization of mTOR

Fluorescence imaging of mTOR translocation for the siRNA screen was based on immunostaining using anti-mTOR and anti-Lamp2 antibodies. Images were acquired with a 20X objective using an automated inverted epifluorescence microscope (ImageXpress 5000A, Axon, or ImageXpressMicro, Molecular Devices). For screening analysis of the 427 genes, a custom-written MatLab script was used to cross-correlate the mTOR and Lamp2 signals in a perinuclear region as a measure for relative co-localization (Figures 1E, 2D). A more quantitative mTOR localization and translocation parameter (a slower but also automated analysis) was based on

identifying local Lamp2 positive vesicles and creating a binary mask and subtract a local background for the analysis of mTOR translocation. Specifically, the nuclei were segmented using a grayscale threshold and a distance matrix was calculated based on how many pixels away from the nucleus. A ring identified by >8 pixels and <20 pixels away from the nucleus was defined as the perinuclear region in which the Lamp2 mask is defined and mTOR intensity is measured. A binary mask of Lamp2 puncta was identified by finding the peak intensity values after using a shifted background mask to subtract non-lysosomal background. This Lamp2 puncta mask was then used to measure the intensity of pixels in the mTOR channel, which is also background-subtracted using a shifted mask. The mTOR pixel values in the Lamp2 puncta per cell are averaged to give a 'relative translocation score' for that cell (Figures 2f, Supplementary Fig. 2b, c and remainder of the figures). To quantify levels of RagA, C and Lamp1 at the lysosome (Fig.6a-f), we substituted RagA, C and Lamp1 for mTOR and used identical automated analysis. For each experiment, 12-25 sites per 96-well were imaged and at least 1,000 cells were analyzed per well and 2-4 wells were included per independent experiment. Statistical analysis was performed either by comparing the averages of control vs. treated wells over independent experiments or comparing averages of transfected cells vs. that of non-transfected cells in the same well.

b. Synergy heatmap analysis of Rag and GPR137B

Figure 5e. HeLa cells were amino acid starved for 10-12hrs, and cells co-expressing Lamp1-Turq and RagC-Venus (n=14004) or GPR137B-Turq and RagC-Venus (n=14207) were binned into 10 equal bins of Turquoise intensities and Venus intensities. Average of mTOR translocation score for each bin is plotted as a blue-yellow heatmap scaled from 50-450. Gray indicates bins where there was insufficient number of cells.

c. FRAP experiments and analysis

All photobleaching experiments were conducted on the 3i imaging system using an 40x objective. Bleaching was set in 515nm for 1s one time in a rectangular area. Images were acquired every 10s and bleaching was set to the 6^{th} frame. For fluorescence recovery measurements, selected lysosomes were tracked manually in ImageJ using Lamp1-Turquoise or GPR137B-Turquoise as a lysosome mask and corresponding average RagC intensity was recorded for each frame. A background region containing no cells was first subtracted from the

raw intensities and then divided by a neighboring non-bleached region. All values were then normalized to the frame immediately before bleaching (5th frame). For bar graphs in Figure 6K, we derived a single measurement by subtracting the fluorescence intensity at frame 10 from frame 5 to represent the relative recovery for each recovery curve, and then averaging the relative recovery for all curves.

Cell Lysis and Immunoprecipitation

For amino acid regulated binding, cells were amino acid starved for 2 hours then amino acids were added back for 10-15 min. Cells were incubated with 1 mg/ mL Dithiobis [succinimidyl propionate] (DSP) for 20 minutes at room temperature then the reaction was quenched by treating cells with 100 mM Tris pH 8.5 for 10 minutes. Cells were lysed in Octyl-glucoside lysis buffer (60 mM n-Octyl-β-D-Glucopyranoside, 50 mM HEPES [pH 7.4], 150 mM NaCl, and protease inhibitor cocktail (Thermo Fisher Scientific) then homogenized with 25-gauge needle and centrifuged at 1100 x g at 4˚C for 5 minutes to remove nuclei. 0.1% SDS was added to the supernatant. The lysate was sonicated briefly; then incubated at 4˚ C for 1 hour followed by centrifugation at 20,000 x g for 60 minutes. The lysates were adjusted to total protein concentration of 0.1 - 0.2 mg/ml and incubated with the FLAG-M2 affinity gel (Sigma Cat#8823) or mouse anti-HA (Pierce Cat#88837 Lot#QJ224632) at 4˚C overnight. The beads were washed three times with ice-cold lysis buffer with 300 mM NaCl then washed twice with lysis buffer. Immunoprecipitated proteins were denatured in urea containing-SDS sample buffer (final concentration of 62.5 mM Tris-HCl, 12.5% Glycerol, 0.01% Bromophenol, 300 mM DTT, 4 M Urea and 3% SDS) at 37˚C for 30 minutes with rotation. The samples were loaded on 4-12% NuPAGE Bis-Tris, 3-8% Tris-Acetate precast gels, or Bolt 4-12% Bis-Tris Plus gels (Life technologies). The signal intensities were analyzed by ImageJ (NIH) and graphed using Prism (GraphPad).

GPR137b-FLAG and GPR137b-HA co-immunoprecipitation

In order to observe amino acid sensitive GPR137b-GPR137b interaction, GPR137b- FLAG and GPR137b-HA were stably co-expressed in MEF RagA/B null or control MEF in low level. To achieve this, upstream ORF of pPBbsr2-GPR137b-FLAG and pLV-EF1a- GPR137B-HA were attenuated by engineering to TTT ([1]). Only earlier passages of cells were used.

Cells were amino acid starved for 3-4 hours and added back for 20 min then DSP crosslinked. GPR137b complex was immunoprecipitated using FLAG-M2 affinity gel at 4˚C overnight. The complex was analyzed by western blot.

Transfection and starvation of HEK293T for co-immunoprecipitation

One day prior to DNA transfection, cells were plated on collagen coated dishes. Next day, GPR137b was transfected using Lipofectamine 2000 (Thermo Fisher Scientific) in Opti-MEM 1 (Thermo Fisher Scientific) overnight. Media was changed to 10% FBS containing DMEM (Thermo Fisher Scientific). Cells were harvested 48 hours after transfection. All co-IP experiments cells were starved and added-back for amino acid in DMEM supplemented with dialyzed FBS. When phosphorylation of S6K was examined (Fig.2k), DMEM without FBS was used. **Zebrafish experiments**

TALEN and CRISPR targeting to Generate Mutations in Zebrafish GPR137B Homologs

The TAL Effector-Nucleotide Targeter 2.0 (Cermak et al., 2011; Doyle et al., 2012) webtool was used to design a pair of transcription activator-like effector nucleases to target *gpr137c, gpr137, and gpr137ba*. The Golden Gate cloning protocol for creating the TALEN plasmids was used (Sanjana et al., 2012). Plasmids were then transcribed using Sp6 mMessage mMachine Kit by Ambion. 400ng of mRNA were injected into 1-cell stage wildtype TL embryos, which were raised to adulthood. To identify founders carrying a null mutation in the germline, we crossed injected fish to wildtype (TL strain) and genotyped a subset of the progeny at 2–3 dpf. The TALEN lesions were given the following names and genotyped using the following primers and restriction assays: ***gpr137c, st117,*** 10bp deletion, forward primer: ttggataagtcggcgtgatag, reverse primer: cgtcctcagagcagaccag, restriction assay using DpnII; ***gpr137, st118,*** 8bp deletion, forward primer: ccatgagcgtcattttcctg, reverse primer: acacccgaatgcatcacac, restriction assay using HpaI; ***gpr137ba, st119,*** 20bp deletion, forward primer: gagcagtgggaagcagaaac, reverse primer: ggtaacgcaaaaccaaccac, restriction assay using: SfaNI. All restriction enzymes cleave the wildtype, but not the mutant allele. Based on the disruption of the restriction site, we identified founders and raised the remaining F1 progeny to adulthood. F1 heterozygous adults for the respective deletions were crossed to the TL strain to establish a stock.

For CRISPR experiments, sgRNAs were designed using CHOPCHOP. The sgRNA was transcribed from the DNA template with T7 polymerase (E2040S, New England Biolabs) and purified using mirVana miRNA isolation kit (AM1560, Ambion). Cas9 protein (Macrolab, Berkeley) and ~300 ng sgRNA were injected into 1-cell stage embryos and embryos were genotyped to detect lesions. The sgRNA used for *gpr137bb* was GGGTCACTACCGGTTGTACC. The efficacy of the sgRNA was determined by sequencing eight individual embryos after PCR using forward primer: GCTATTCCCAGCCACGTGTTC and reverse primer: CACAGGAGATACAGCTCAGTGC

Neutral Red and Lysotracker Red Staining of Live Zebrafish Larvae

Larvae at 4 dpf were incubated in a 1:100 dilution of LysoTracker Red DND-99 (Invitrogen) in embryo water at 28.5°C for 45 min, washed twice with embryo water, mounted in 1.5% LMP agarose and imaged with a Zeiss confocal microscope. For the neutral red assay, larvae at 5 dpf were incubated in 2.5 μg/ml neutral red at 28.5°C for 2.5 hours, washed twice with embryo water, mounted in 1.5% LMP agarose and analyzed using a dissecting microscope.

Particle Analysis in ImageJ

LysoTracker Red-stained images are thresholded to generate a binary image and despeckled. “Analyze Particles” with a setting of area >30 pixels was used to generate overlays and measure the area of LysoTracker Red stained puncta.

qRT-PCR

Zebrafish larvae were obtained from a cross between *gpr137c+/-*; *gpr137+/-*; *gpr137ba-/-* male X *gpr137c-/-*; *gpr137+/-*; *gpr137ba+/-* female adults. At 5 days post fertilization, larvae were anesthetized with tricaine. DNA was prepared from tail fins of individual fish, and the remaining portion of each fish was snap frozen on dry ice. The genotypes of each animal were determined by a PCR assay for the *gpr137ba* lesion and the frozen larvae were pooled based on the genotype for *gpr137ba*. Three batches of 15-16 embryos that were either heterozygous (*gpr137ba+/-*) or homozygous (*gpr137ba-/-*) mutants were pooled separately to obtain biological triplicates. Total RNA was extracted from pooled embryos using the RNAeasy kit (QIAGEN). cDNA was synthesized using iScript supermix (Biorad). qPCR was performed with SsoAdvancedTM Universal SYBR Green Supermix (Bio-Rad) on the Bio-Rad CFX384 Real-Time PCR Detection

System. All experiments were done in biological and technical triplicates. Transcript levels were normalized to eif1-α (Shen et al., 2016; Shiau et al., 2013). Relative mRNA levels were calculated using ΔΔCT.

SUPPLEMENTAL REFERENCES

Carpenter, A.E., Jones, T.R., Lamprecht, M.R., Clarke, C., Kang, I.H., Friman, O., Guertin, D.A., Chang, J.H., Lindquist, R.A., Moffat, J., et al. (2006). CellProfiler: image analysis software for identifying and quantifying cell phenotypes. Genome Biol. *7*, R100.

Cermak, T., Doyle, E.L., Christian, M., Wang, L., Zhang, Y., Schmidt, C., Baller, J.A., Somia, N. V, Bogdanove, A.J., and Voytas, D.F. (2011). Efficient design and assembly of custom TALEN and other TAL effector-based constructs for DNA targeting. Nucleic Acids Res. *39*, e82.

Doyle, E.L., Booher, N.J., Standage, D.S., Voytas, D.F., Brendel, V.P., Vandyk, J.K., and Bogdanove, A.J. (2012). TAL Effector-Nucleotide Targeter (TALE-NT) 2.0: tools for TAL effector design and target prediction. Nucleic Acids Res. *40*, W117-22.

Galvez, T., Teruel, M.N., Heo, W. Do, Jones, J.T., Kim, M.L., Liou, J., Myers, J.W., and Meyer, T. (2007). siRNA screen of the human signaling proteome identifies the PtdIns(3,4,5)P3-mTOR signaling pathway as a primary regulator of transferrin uptake. Genome Biol. *8*, R142.

Paulsen, R.D., Soni, D. V, Wollman, R., Hahn, A.T., Yee, M.-C., Guan, A., Hesley, J.A., Miller, S.C., Cromwell, E.F., Solow-Cordero, D.E., et al. (2009). A genome-wide siRNA screen reveals diverse cellular processes and pathways that mediate genome stability. Mol. Cell *35*, 228–239.

Sanjana, N.E., Cong, L., Zhou, Y., Cunniff, M.M., Feng, G., and Zhang, F. (2012). A transcription activator-like effector toolbox for genome engineering. Nat. Protoc. *7*, 171–192.

1.Ferreira, J. P., Overton, K. W. & Wang, C. L. Tuning gene expression with synthetic upstream open reading frames. *Proc. Natl. Acad. Sci. U.S.A.* **110,** 11284–11289 (2013).

Meireles, A.M., Shen, K., Zoupi, L., Iyer, H., Bouchard, E.L., Williams, A., Talbot, W.S., 2018. The Lysosomal Transcription Factor TFEB Represses Myelination Downstream of the Rag-Ragulator Complex. Dev. Cell 47, 319–330.e5. doi:10.1016/j.devcel.2018.10.003

Napolitano, G., Ballabio, A., 2016. TFEB at a glance. J Cell Sci 129, 2475–2481. doi:10.1242/jcs.146365

Shen, K., Sidik, H., Talbot, W.S., 2016. The Rag-Ragulator Complex Regulates Lysosome Function and Phagocytic Flux in Microglia. Cell Rep 14, 547–559. doi:10.1016/j.celrep.2015.12.055

Shiau, C.E., Monk, K.R., Joo, W., Talbot, W.S., 2013. An anti-inflammatory NOD-like receptor is required for microglia development. Cell Rep 5, 1342–1352. doi:10.1016/j.celrep.2013.11.004

Figure 1

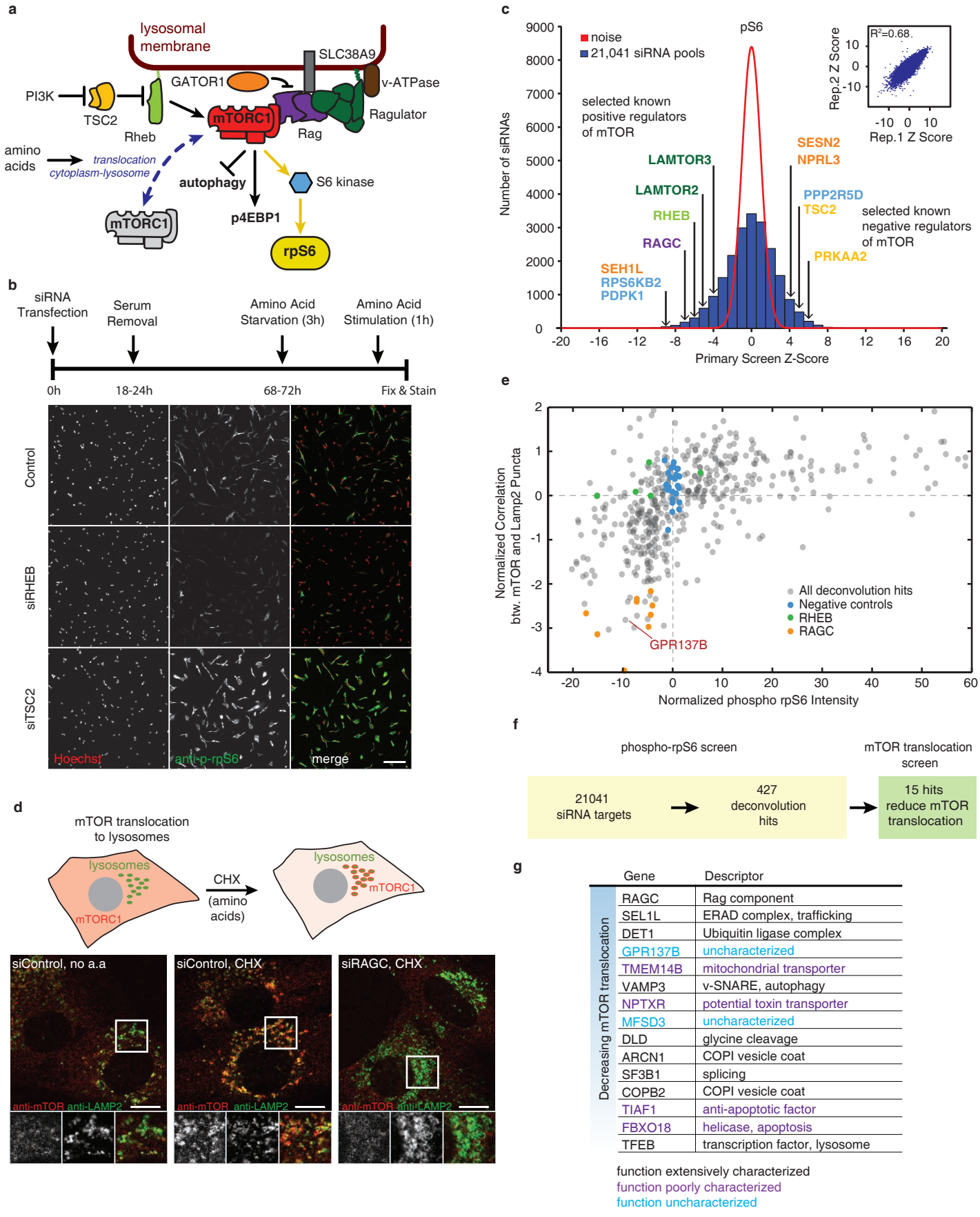
a
lysosomal membrane
SLC38A9
GATOR1
v-ATPase
PI3K
TSC2
Rheb
mTORC1
Rag
Ragulator
amino acids
translocation cytoplasm-lysosome
autophagy
S6 kinase
mTORC1
p4EBP1
rpS6
b
siRNA Transfection
Serum Removal
Amino Acid Starvation (3h)
Amino Acid Stimulation (1h)
0h
18-24h
68-72h
Fix & Stain
Control
siRHEB
siTSC2
Hoechst
anti-p-rpS6
merge
c
noise
21,041 siRNA pools
pS6
selected known positive regulators of mTOR
SESN2
NPRL3
LAMTOR3
LAMTOR2
RHEB
RAGC
PPP2R5D
TSC2
selected known negative regulators of mTOR
PRKAA2
SEH1L
RPS6KB2
PDPK1
Number of siRNAs
Primary Screen Z-Score
R²=0.68
Rep.2 Z Score
Rep.1 Z Score
d
mTOR translocation to lysosomes
lysosomes
mTORC1
CHX (amino acids)
siControl, no a.a
siControl, CHX
siRAGC, CHX
anti-mTOR anti-LAMP2
e
Normalized Correlation btw. mTOR and Lamp2 Puncta
Normalized phospho rpS6 Intensity
All deconvolution hits
Negative controls
RHEB
RAGC
GPR137B
f
phospho-rpS6 screen
mTOR translocation screen
21041 siRNA targets
427 deconvolution hits
15 hits reduce mTOR translocation
g
Decreasing mTOR translocation
Gene
Descriptor
RAGC
Rag component
SEL1L
ERAD complex, trafficking
DET1
Ubiquitin ligase complex
GPR137B
uncharacterized
TMEM14B
mitochondrial transporter
VAMP3
v-SNARE, autophagy
NPTXR
potential toxin transporter
MFSD3
uncharacterized
DLD
glycine cleavage
ARCN1
COPI vesicle coat
SF3B1
splicing
COPB2
COPI vesicle coat
TIAF1
anti-apoptotic factor
FBXO18
helicase, apoptosis
TFEB
transcription factor, lysosome
function extensively characterized
function poorly characterized
function uncharacterized

Figure 2

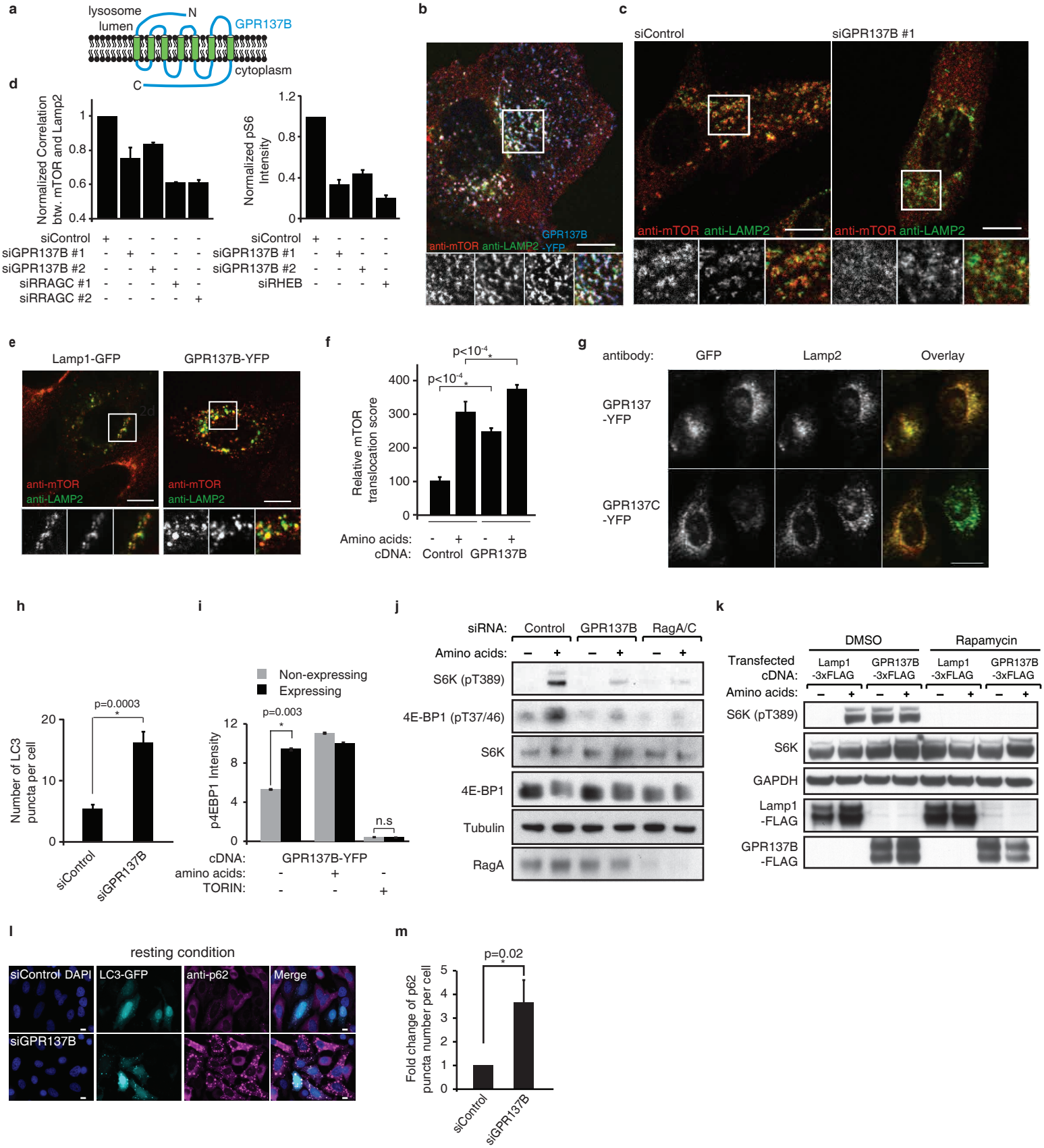
a
lysosome lumen
N
GPR137B
cytoplasm
C
b
GPR137B
anti-mTOR anti-LAMP2 -YFP
c
siControl
siGPR137B #1
anti-mTOR anti-LAMP2
anti-mTOR anti-LAMP2
d
Normalized Correlation btw. mTOR and Lamp2
siControl + - - - -
siGPR137B #1 - + - - -
siGPR137B #2 - - + - -
siRRAGC #1 - - - + -
siRRAGC #2 - - - - +
Normalized pS6 Intensity
siControl + - - -
siGPR137B #1 - + - -
siGPR137B #2 - - + -
siRHEB - - - +
e
Lamp1-GFP
GPR137B-YFP
anti-mTOR anti-LAMP2
anti-mTOR anti-LAMP2
f
p<10-4 *
p<10-4 *
Relative mTOR translocation score
Amino acids: - + - +
cDNA: Control GPR137B
g
antibody: GFP Lamp2 Overlay
GPR137 -YFP
GPR137C -YFP
h
p=0.0003 *
Number of LC3 puncta per cell
siControl
siGPR137B
i
Non-expressing
Expressing
p=0.003 *
n.s
p4EBP1 Intensity
cDNA: GPR137B-YFP
amino acids: - + -
TORIN: - - +
j
siRNA: Control GPR137B RagA/C
Amino acids: – + – + – +
S6K (pT389)
4E-BP1 (pT37/46)
S6K
4E-BP1
Tubulin
RagA
k
DMSO
Rapamycin
Transfected cDNA: Lamp1 -3xFLAG GPR137B -3xFLAG Lamp1 -3xFLAG GPR137B -3xFLAG
Amino acids: – + – + – + – +
S6K (pT389)
S6K
GAPDH
Lamp1 -FLAG
GPR137B -FLAG
l
resting condition
siControl DAPI
LC3-GFP
anti-p62
Merge
siGPR137B
m
p=0.02 *
Fold change of p62 puncta number per cell
siControl
siGPR137B

Figure 3

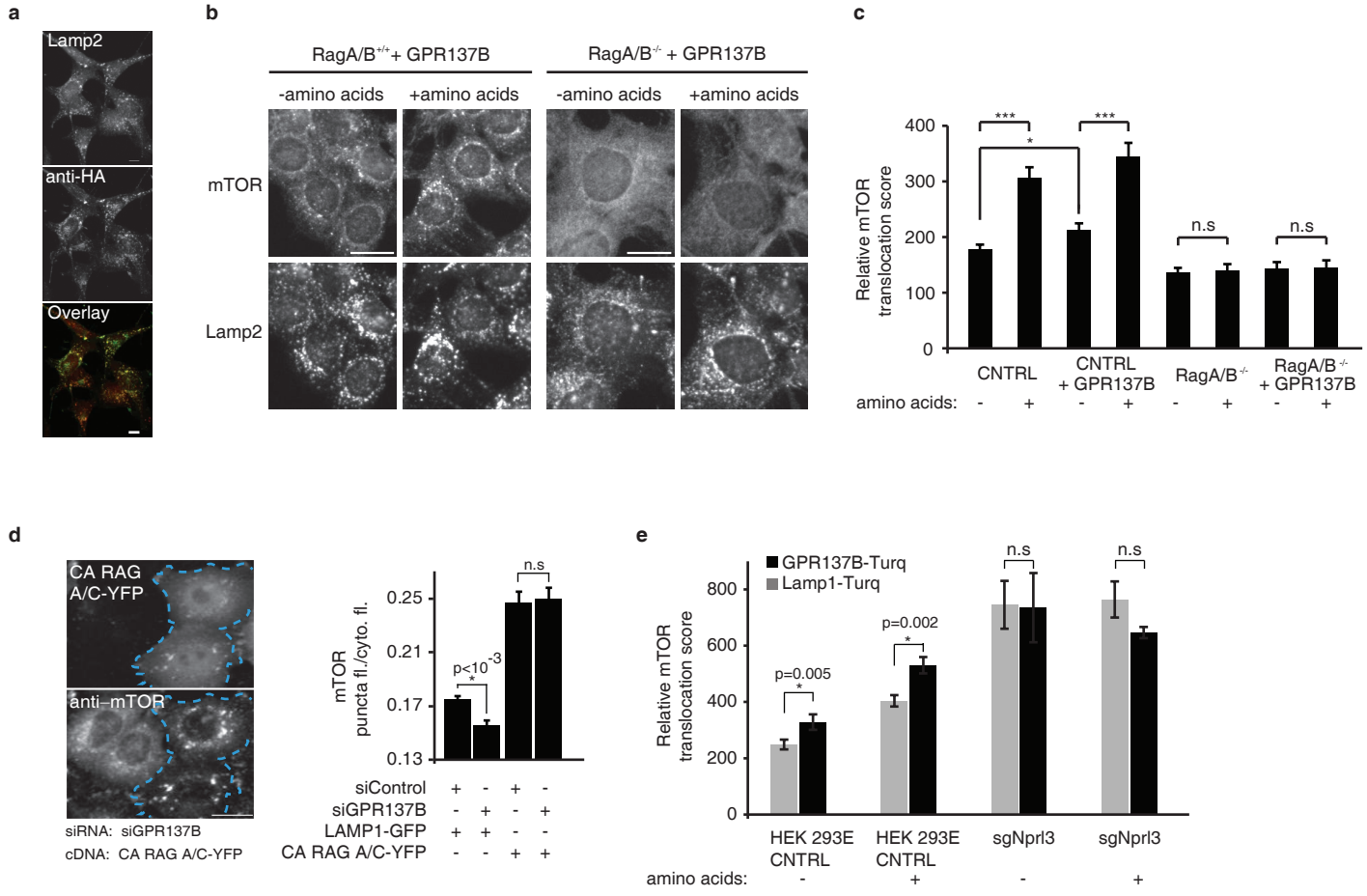
a
Lamp2
anti-HA
Overlay
b
RagA/B+/+ + GPR137B
RagA/B-/- + GPR137B
-amino acids
+amino acids
-amino acids
+amino acids
mTOR
Lamp2
c
Relative mTOR translocation score
400
300
200
100
0
***
*
***
n.s
n.s
CNTRL
CNTRL + GPR137B
RagA/B-/-
RagA/B-/- + GPR137B
amino acids: - + - + - + - +
d
CA RAG A/C-YFP
anti–mTOR
siRNA: siGPR137B
cDNA: CA RAG A/C-YFP
mTOR puncta fl./cyto. fl.
0.25
0.21
0.17
0.13
p<10-3
*
n.s
siControl + - + -
siGPR137B - + - +
LAMP1-GFP + + - -
CA RAG A/C-YFP - - + +
e
GPR137B-Turq
Lamp1-Turq
Relative mTOR translocation score
800
600
400
200
0
p=0.005
p=0.002
*
*
n.s
n.s
HEK 293E CNTRL
HEK 293E CNTRL
sgNprl3
sgNprl3
amino acids: - + - +

Figure 4

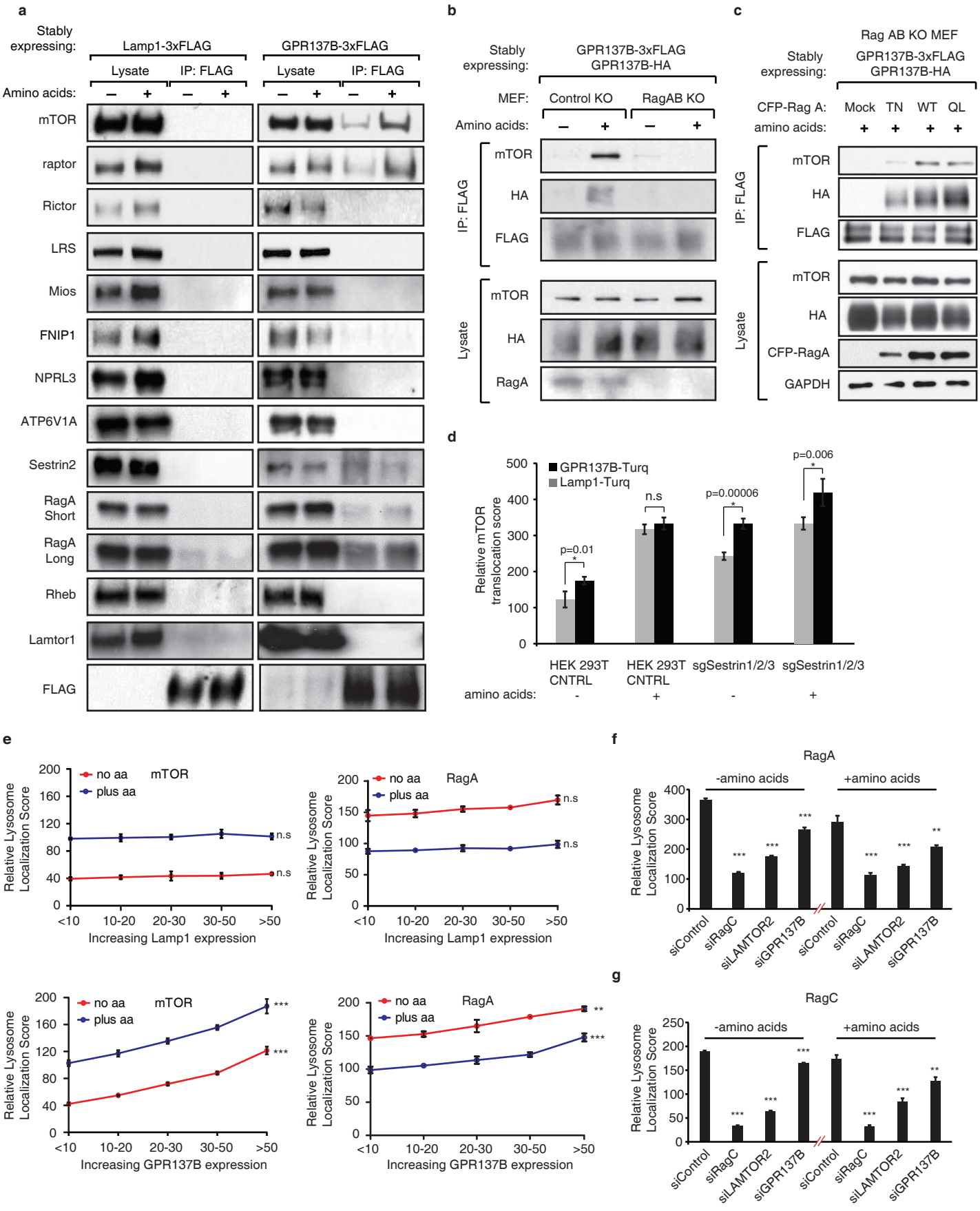
a
Stably expressing:
Lamp1-3xFLAG
GPR137B-3xFLAG
Lysate
IP: FLAG
Amino acids:
mTOR
raptor
Rictor
LRS
Mios
FNIP1
NPRL3
ATP6V1A
Sestrin2
RagA Short
RagA Long
Rheb
Lamtor1
FLAG
b
Stably expressing:
GPR137B-3xFLAG GPR137B-HA
MEF:
Control KO
RagAB KO
Amino acids:
IP: FLAG
mTOR
HA
FLAG
Lysate
mTOR
HA
RagA
c
Rag AB KO MEF
Stably expressing:
GPR137B-3xFLAG GPR137B-HA
CFP-Rag A:
Mock
TN
WT
QL
amino acids:
IP: FLAG
mTOR
HA
FLAG
Lysate
mTOR
HA
CFP-RagA
GAPDH
d
GPR137B-Turq
Lamp1-Turq
Relative mTOR translocation score
p=0.01
n.s
p=0.00006
p=0.006
HEK 293T CNTRL
HEK 293T CNTRL
sgSestrin1/2/3
sgSestrin1/2/3
amino acids:
e
no aa
plus aa
mTOR
RagA
Relative Lysosome Localization Score
Increasing Lamp1 expression
Increasing GPR137B expression
n.s
f
RagA
-amino acids
+amino acids
siControl
siRagC
siLAMTOR2
siGPR137B
g
RagC

Figure 5

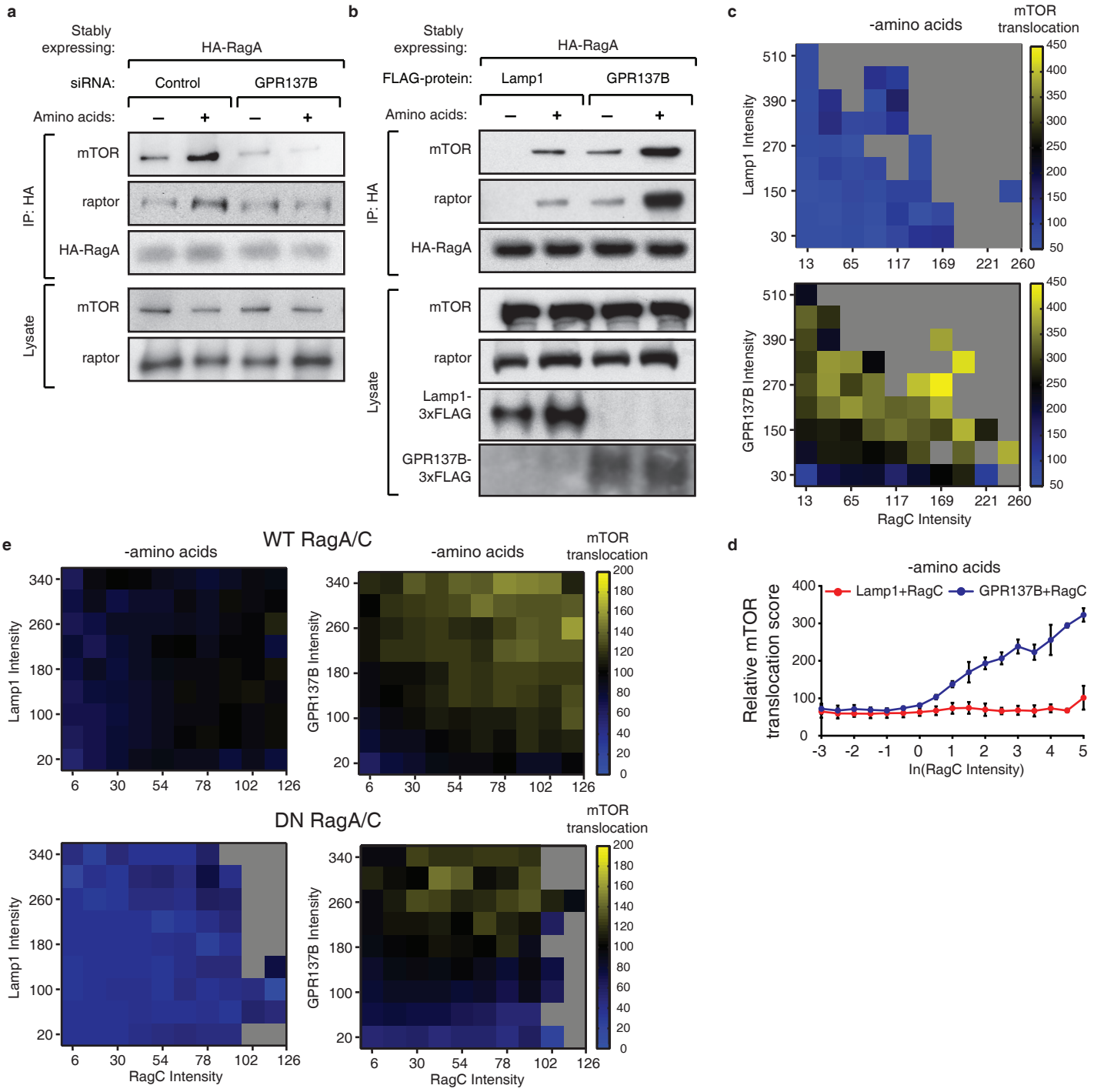
a
Stably expressing:
HA-RagA
siRNA:
Control
GPR137B
Amino acids:
– + – +
IP: HA
mTOR
raptor
HA-RagA
Lysate
mTOR
raptor
b
Stably expressing:
HA-RagA
FLAG-protein:
Lamp1
GPR137B
Amino acids:
– + – +
IP: HA
mTOR
raptor
HA-RagA
Lysate
mTOR
raptor
Lamp1-3xFLAG
GPR137B-3xFLAG
c
-amino acids
mTOR translocation
Lamp1 Intensity
GPR137B Intensity
RagC Intensity
d
-amino acids
Lamp1+RagC
GPR137B+RagC
Relative mTOR translocation score
ln(RagC Intensity)
e
WT RagA/C
-amino acids
mTOR translocation
Lamp1 Intensity
GPR137B Intensity
DN RagA/C
RagC Intensity

Figure 6

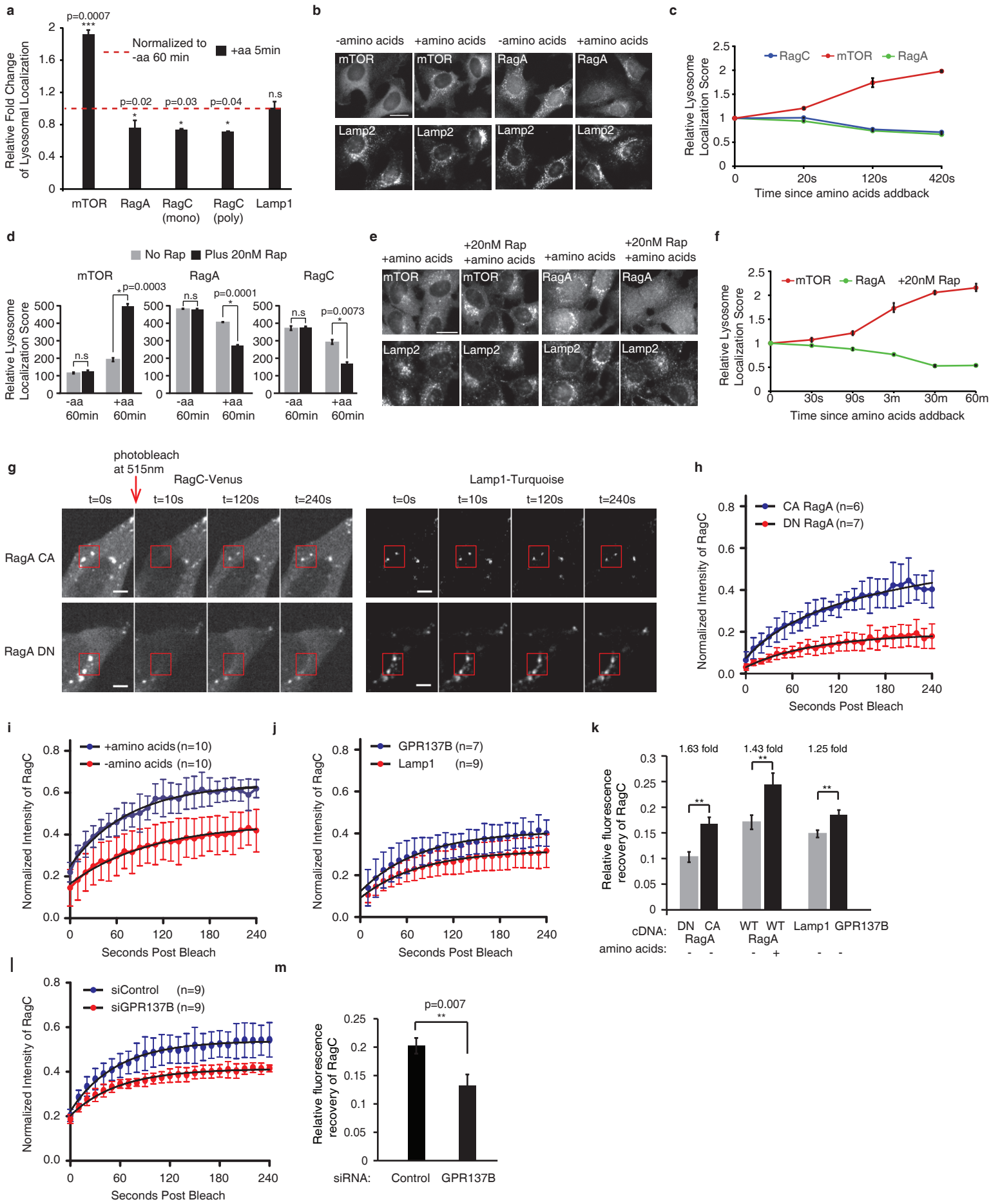
a
p=0.0007
***
Normalized to -aa 60 min
+aa 5min
p=0.02
p=0.03
p=0.04
n.s
Relative Fold Change of Lysosomal Localization
mTOR
RagA
RagC (mono)
RagC (poly)
Lamp1
b
-amino acids
+amino acids
-amino acids
+amino acids
mTOR
RagA
Lamp2
c
RagC
mTOR
RagA
Relative Lysosome Localization Score
Time since amino acids addback
0
20s
120s
420s
d
No Rap
Plus 20nM Rap
mTOR
RagA
RagC
p=0.0003
p=0.0001
p=0.0073
n.s
Relative Lysosome Localization Score
-aa 60min
+aa 60min
e
+amino acids
+20nM Rap +amino acids
mTOR
RagA
Lamp2
f
mTOR
RagA
+20nM Rap
Relative Lysosome Localization Score
Time since amino acids addback
0
30s
90s
3m
30m
60m
g
photobleach at 515nm
RagC-Venus
Lamp1-Turquoise
t=0s
t=10s
t=120s
t=240s
RagA CA
RagA DN
h
CA RagA (n=6)
DN RagA (n=7)
Normalized Intensity of RagC
Seconds Post Bleach
i
+amino acids (n=10)
-amino acids (n=10)
Normalized Intensity of RagC
Seconds Post Bleach
j
GPR137B (n=7)
Lamp1 (n=9)
Normalized Intensity of RagC
Seconds Post Bleach
k
1.63 fold
1.43 fold
1.25 fold
Relative fluorescence recovery of RagC
cDNA:
DN RagA
CA RagA
WT RagA
WT RagA
Lamp1
GPR137B
amino acids:
l
siControl (n=9)
siGPR137B (n=9)
Normalized Intensity of RagC
Seconds Post Bleach
m
p=0.007
**
Relative fluorescence recovery of RagC
siRNA:
Control
GPR137B

Figure 7

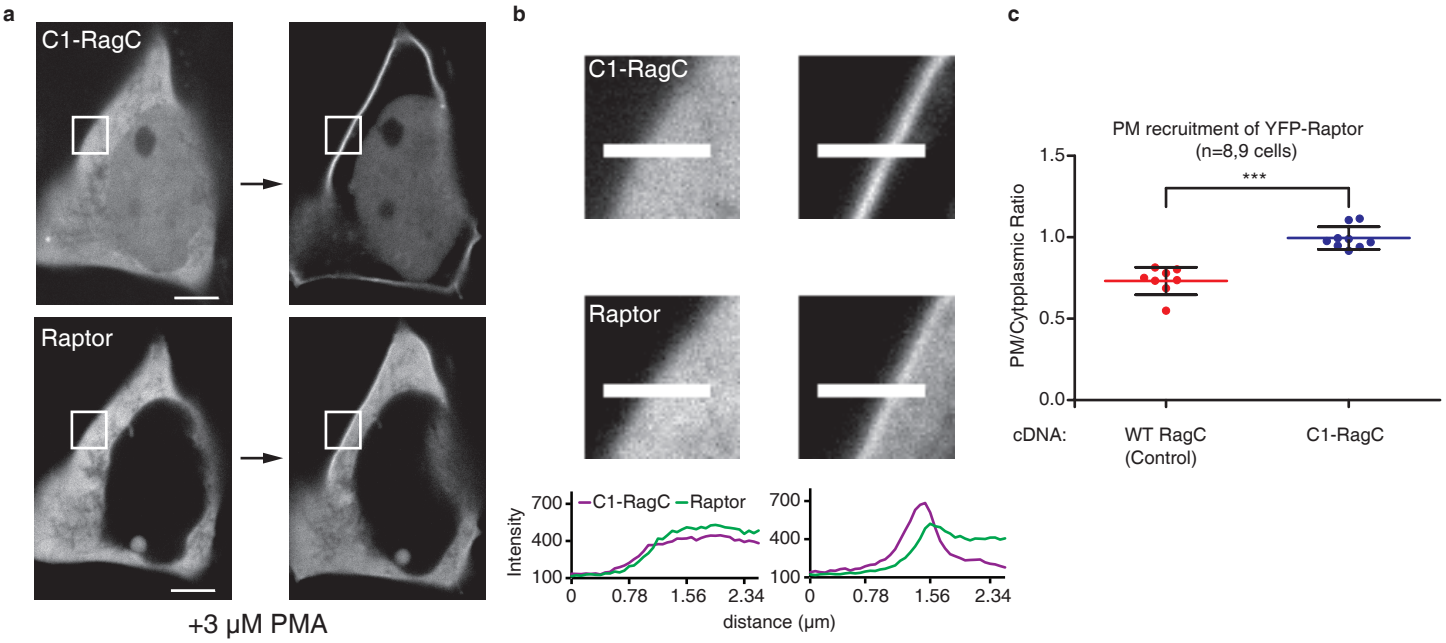
a
C1-RagC
Raptor
+3 μM PMA
b
C1-RagC
Raptor
Intensity
C1-RagC
Raptor
700
400
100
0
0.78
1.56
2.34
distance (μm)
c
PM recruitment of YFP-Raptor
(n=8,9 cells)
***
PM/Cytpplasmic Ratio
1.5
1.0
0.5
0.0
cDNA:
WT RagC
(Control)
C1-RagC

Figure 8

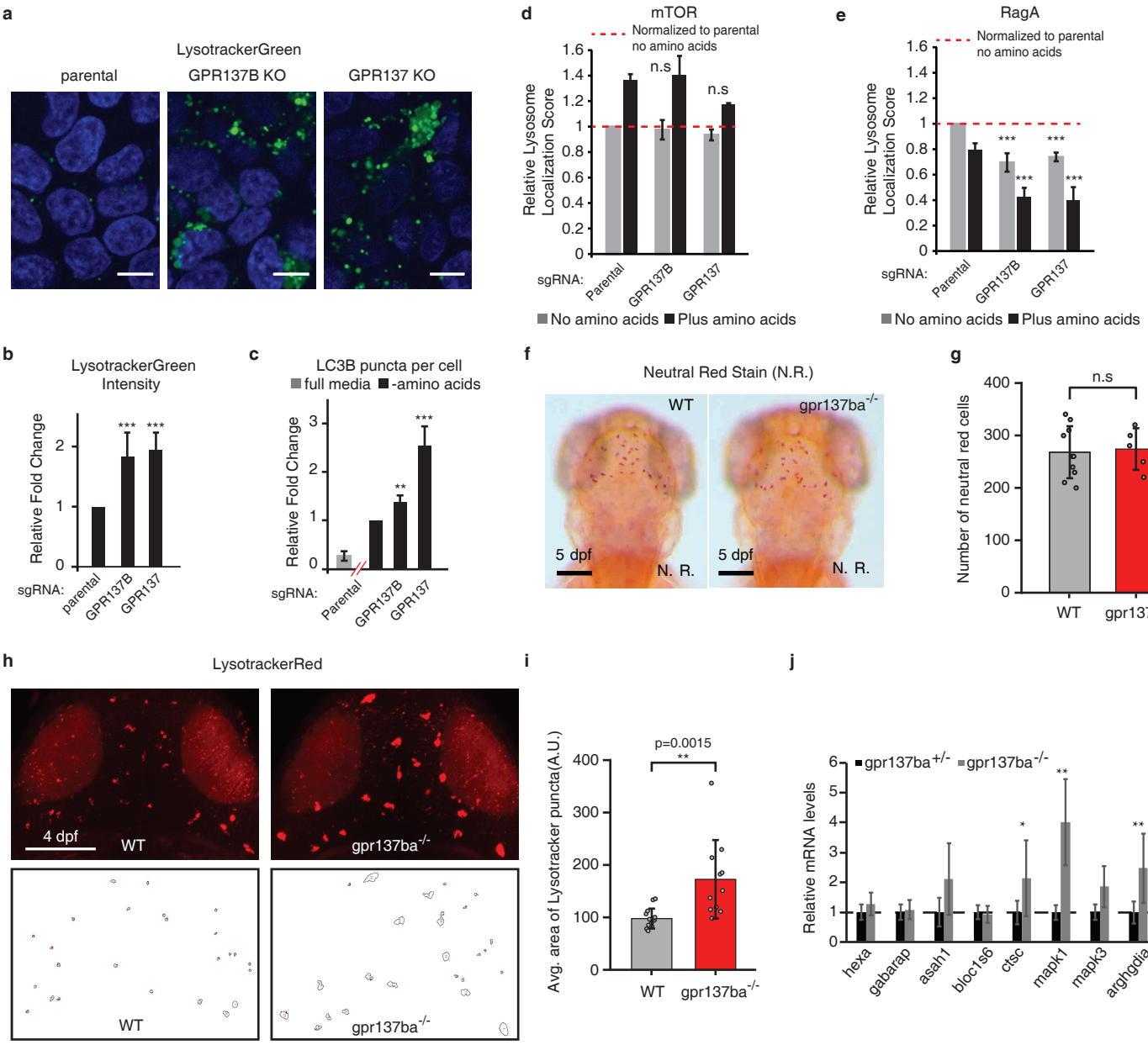
a
LysotrackerGreen
parental
GPR137B KO
GPR137 KO
d
mTOR
Normalized to parental no amino acids
Relative Lysosome Localization Score
n.s
n.s
sgRNA:
Parental
GPR137B
GPR137
No amino acids
Plus amino acids
e
RagA
Normalized to parental no amino acids
Relative Lysosome Localization Score
***
***
***
***
sgRNA:
Parental
GPR137B
GPR137
No amino acids
Plus amino acids
b
LysotrackerGreen Intensity
Relative Fold Change
***
***
sgRNA:
parental
GPR137B
GPR137
c
LC3B puncta per cell
full media
-amino acids
Relative Fold Change
**
***
sgRNA:
Parental
GPR137B
GPR137
f
Neutral Red Stain (N.R.)
WT
gpr137ba-/-
5 dpf
N. R.
5 dpf
N. R.
g
Number of neutral red cells
n.s
WT
gpr137ba-/-
h
LysotrackerRed
4 dpf
WT
gpr137ba-/-
WT
gpr137ba-/-
i
Avg. area of Lysotracker puncta(A.U.)
p=0.0015
**
WT
gpr137ba-/-
j
Relative mRNA levels
gpr137ba+/-
gpr137ba-/-
*
**
**
**
hexa
gabarap
asah1
bloc1s6
ctsc
mapk1
mapk3
arghgdia
dusp1
sqstm